

Analysis of the accuracy and convergence of equation-free projection to a slow manifold

May 14, 2007

A. Zagaris^{1,2}, C. W. Gear^{3,4}, T. J. Kaper⁵, I. G. Kevrekidis^{3,6}

- 1 Department of Mathematics, University of Amsterdam, Amsterdam, The Netherlands.
 2 Modeling, Analysis and Simulation, Centrum voor Wiskunde en Informatica, Amsterdam, The Netherlands.
 3 Department of Chemical Engineering, Princeton University, Princeton, NJ 08544;
 4 NEC Laboratories USA, retired;
 5 Department of Mathematics and Center for BioDynamics, Boston University, Boston, MA 02215;
 6 Program in Applied and Computational Mathematics, Princeton University, Princeton, NJ 08544;

Abstract

In [C. W. Gear, T. J. Kaper, I. G. Kevrekidis, and A. Zagaris, Projecting to a Slow Manifold: Singularly Perturbed Systems and Legacy Codes, *SIAM J. Appl. Dyn. Syst.* **4** (2005) 711–732], we developed a class of iterative algorithms within the context of equation-free methods to approximate low-dimensional, attracting, slow manifolds in systems of differential equations with multiple time scales. For user-specified values of a finite number of the observables, the m -th member of the class of algorithms ($m = 0, 1, \dots$) finds iteratively an approximation of the appropriate zero of the $(m + 1)$ -st time derivative of the remaining variables and uses this root to approximate the location of the point on the slow manifold corresponding to these values of the observables. This article is the first of two articles in which the accuracy and convergence of the iterative algorithms are analyzed. Here, we work directly with explicit fast–slow systems, in which there is an explicit small parameter, ε , measuring the separation of time scales. We show that, for each $m = 0, 1, \dots$, the fixed point of the iterative algorithm approximates the slow manifold up to and including terms of $\mathcal{O}(\varepsilon^m)$. Moreover, for each m , we identify explicitly the conditions under which the m -th iterative algorithm converges to this fixed point. Finally, we show that when the iteration is unstable (or converges slowly) it may be stabilized (or its convergence may be accelerated) by application of the Recursive Projection Method. Alternatively, the Newton–Krylov Generalized Minimal Residual Method may be used. In the subsequent article, we will consider the accuracy and convergence of the iterative algorithms for a broader class of systems—in which there need not be an explicit small parameter—to which the algorithms also apply.

1 Introduction

The long-term dynamics of many complex chemical, physical, and biological systems simplify when a low-dimensional, attracting, invariant slow manifold is present. Such a slow manifold attracts all nearby initial data exponentially, and the reduced dynamics on it govern the long term evolution of the full system. More specifically, a slow manifold is parametrized by observables which are typically slow variables or functions of variables. All nearby system trajectories decompose naturally into a fast component that contracts exponentially toward the slow manifold and a slow component which obeys the reduced system dynamics on the manifold. In this sense, the fast variables become slaved to the observables, and knowledge of the slow manifold and of the reduced dynamics on it suffices to determine the full long-term system dynamics.

The identification and approximation of slow manifolds is usually achieved by employing a reduction method. We briefly list a number of these: Intrinsic Low Dimensional Manifold (ILDm), Computational Singular Perturbation (CSP), Method of Invariant Manifold (MIM), Approximate Inertial Manifold approaches, and Fraser-Roussel iteration, and we refer the reader to [4, 8] for a more extensive listing.

1.1 A class of iterative algorithms based on the zero-derivative principle

In [4], we developed a class of iterative algorithms to locate slow manifolds for systems of Ordinary Differential Equations (ODEs) of the form

$$\begin{aligned} u' &= p(u, v), & u &\in \mathbf{R}^{N_s}, \\ v' &= q(u, v), & v &\in \mathbf{R}^{N_f}, \end{aligned} \tag{1.1}$$

where $N_s + N_f \equiv N$. We treated the variables u as the observables (that is, as parametrizing the slow manifold we are interested in), and we assumed that there exists an N_s -dimensional, attracting, invariant, slow manifold \mathcal{L} , which is given locally by the graph of a function $v = v(u)$. However, we emphasize that we did not need explicit knowledge of which variables are fast and which are slow, only that the variables u suffice to parametrize \mathcal{L} .

To leading order, the location of a slow manifold \mathcal{L} is obtained by setting $v' = 0$, *i.e.*, by solving $q(u, v) = 0$ for v . Of course, the manifold defined by this equation is in general not an invariant slow manifold under the flow of the full system (1.1). This is only approximately true, since higher-order derivatives with respect to the (fast) time t are, in general, large on it. If one requires that v'' vanishes, then the

solutions with initial conditions at the points defined by this condition depend only on the slow time to one order higher, as v' also remains bounded in the vicinity of this manifold. Similarly, demanding that successively higher-order time derivatives vanish, we obtain manifolds where all time derivatives of lower order remain bounded. The solutions with these initial conditions depend only on the slow time to successively higher order and thus approximate, also to successively higher order, solutions on the slow manifold. In other words, demanding that time derivatives of successively higher order vanish, we filter out the fast dynamics of the solutions to successively higher orders. In this manner, the approximation of the slow manifold \mathcal{L} is improved successively, as well. This idea may be traced back at least to the work of Kreiss [1, 11, 12], who studied systems with rapid oscillations (asymptotically large frequencies) and introduced the bounded derivative principle to find approximations of slow manifolds as the sets of points at which the derivatives are bounded (not large). The requirement here that the derivatives with respect to the (fast) time t vanish is the analog for systems (1.1) with asymptotically stable slow manifolds. A similar idea was introduced independently by Lorenz in [13], where he used a simple functional iteration scheme to approximate the zero of the first derivative, then used the converged value of this scheme to initialize a similar scheme that approximates the zero of the second derivative, and so on until successive zeroes were found to be virtually identical. See also [3] and [6] for other works in which a similar condition is employed.

The elements of the class of iterative algorithms introduced in [4] are indexed by $m = 0, 1, \dots$. The m -th algorithm is designed to locate, for any fixed value of the observable u_0 , an appropriate solution, $v = v_m(u_0)$, of the $(m + 1)$ -st derivative condition

$$\left(\frac{d^{m+1}v}{dt^{m+1}} \right) (u_0, v) = 0. \quad (1.2)$$

Here, the time derivatives are evaluated along solutions of (1.1). In general, since condition (1.2) constitutes a system of N_f nonlinear algebraic equations, the solution $v_m(u_0)$ cannot be computed explicitly. Also, the explicit form of (1.1), and thus also an analytic formula for the $(m + 1)$ -st time derivative in Eq. (1.2), may be unavailable (*e.g.*, in Equation-Free or legacy code applications). In this case, a numerical approximation for it has to be used. The m -th algorithm in the class generates an approximation $v_m^\#$ of $v_m(u_0)$, rather than $v_m(u_0)$ itself, using either an analytic formula for the time derivative or a finite difference approximation for it. In either case, the approximation $v_m^\#$ to $v_m(u_0)$ is determined through an explicit functional iteration scheme, which we now introduce.

The $m = 0$ algorithm is defined by the map $\tilde{F}_0 : \mathbf{R}^{N_f} \rightarrow \mathbf{R}^{N_f}$

$$\tilde{F}_0(v) = v + H \left(\frac{dv}{dt} \right) (u_0, v),$$

where H , which we label as the iterative step size, is an arbitrary positive number whose magnitude we fix below for stability reasons. We initialize the iteration with some value $v^{(1)}$ and generate the sequence

$$\left\{ v^{(r+1)} \equiv \tilde{F}_0(v^{(r)}) \mid r = 1, 2, \dots \right\}.$$

The functional iteration is terminated when $\|v^{(r+1)} - v^{(r)}\| < \text{TOL}_0$, for some $r \geq 1$ and a prescribed tolerance TOL_0 . The output of this zeroth algorithm is the last member, $v_0^\#$, of the sequence $\{v^{(r+1)}\}$.

Next, the $m = 1$ algorithm is defined by the map $\tilde{F}_1 : \mathbf{R}^{\text{Nf}} \rightarrow \mathbf{R}^{\text{Nf}}$,

$$\tilde{F}_1(v) = v - H^2 \left(\frac{d^2 v}{dt^2} \right) (u_0, v),$$

initialized with some value $v^{(1)}$. It generates the sequence

$$\left\{ v^{(r+1)} \equiv \tilde{F}_1(v^{(r)}) \mid r = 1, 2, \dots \right\}$$

and the functional iteration is terminated when $\|v^{(r+1)} - v^{(r)}\| < \text{TOL}_1$, for some $r \geq 1$ and for a prescribed tolerance TOL_1 . The output of this first algorithm is the last member, $v_1^\#$, of the sequence $\{v^{(r+1)}\}$.

The algorithm with general m is defined by the map $\tilde{F}_m : \mathbf{R}^{\text{Nf}} \rightarrow \mathbf{R}^{\text{Nf}}$,

$$\tilde{F}_m(v) = v - (-H)^{m+1} \left(\frac{d^{m+1} v}{dt^{m+1}} \right) (u_0, v), \quad (1.3)$$

seeded with some value $v^{(1)}$. It generates the sequence

$$\left\{ v^{(r+1)} \equiv \tilde{F}_m(v^{(r)}) \mid r = 1, 2, \dots \right\}.$$

Here also, one prescribes a tolerance TOL_m and terminates the iteration procedure when $\|v^{(r+1)} - v^{(r)}\| < \text{TOL}_m$ for some $r \geq 1$. The output of this m -th algorithm is the last member of the sequence $\{v^{(r+1)}\}$, denoted by $v_m^\#$.

As we show in this article, not only is the point $(u_0, v_m^\#)$ of interest for each individual m because it *approximates* $(u_0, v(u_0))$, but the entire sequence $\{(u_0, v_m^\#)\}_m$ is also of interest because it *converges* to $(u_0, v(u_0))$ with a suitably convergent sequence $\{\text{TOL}_m\}$. Hence, the latter point can be approximated arbitrarily well by members of that sequence, and the class of algorithms may be used as an integrated sequence of algorithms in which the output $v_m^\#$ of the m -th algorithm can be used to initialize the $(m + 1)$ -st algorithm. Of course, other initializations are also possible, and we have carried out the analysis here in a manner that is independent of which choice one makes.

This class of iterative algorithms was applied in [4] to three examples: the two-dimensional Michaelis–Menten mechanism for which the one-dimensional slow manifold can be computed analytically to arbitrary precision, a five-dimensional nonlinear system with an explicitly computable two-dimensional slow manifold, and a seven-dimensional hydrogen-oxygen system with quadratic nonlinearities for which the manifold is not known explicitly. In the context of these three examples, we found that, for all of the values of m that we worked with, the m -th algorithm converged at an exponential rate to a fixed point. Moreover, in the two examples where the slow manifold can be computed, we also found that, for each algorithm, this fixed point is very close to the actual point on the slow manifold. In addition to showing the m -th algorithm converged for each m that we worked with, we also showed that the class of algorithms may be used in the integrated manner stated above. The closeness of the approximation to $(u_0, v(u_0))$ improved as we increased the order m of the algorithm used.

More recently, van Leemput *et al.* [16] employed the first ($m = 0$) algorithm in the class to initialize Lattice Boltzmann Models (LBM) from sets of macroscopic data in a way that eliminates the stiff dynamics triggered by a bad initialization. They showed that the algorithm they derived converges unconditionally to a fixed point close to a slow manifold, and they used the algorithm to couple a LBM to a reaction-diffusion equation along the interface with good results [17].

Our motivation for introducing this class of iterative algorithms in [4] was two-fold. First, we wanted a method that can be implemented in the context of legacy codes. In other words, we wanted this reduction method to be implementable even when one has no explicit form for the components p and q of the vector field, but only a black-box integrator (timestepper). This feature renders the method “equation-free” [10] and makes its implementation possible in these settings. Second, it was essential for us that they preserve the user-specified value of the observables, say $u = u_0$, at each iteration. In this way, the output of the algorithm is an approximation of the point $(u_0, v(u_0))$ on the manifold \mathcal{L} of that same value u_0 of the observables. Also, in this way, the ‘lifting’ step in projective integration of [5] is naturally facilitated.

It is worth noting that one really only needs to require that the time derivatives are sufficiently small, although we work with the zero-derivative condition (1.2) for definiteness.

1.2 Iterative algorithms based on the zero-derivative principle for explicit fast–slow systems

A central assumption that we made in [4] is that we work with systems (1.1) for which there exists a smooth and invertible coordinate change

$$z = z(w) \quad \text{with inverse} \quad w = w(z), \quad (1.4)$$

where $w = (u, v)$ and $z = (x, y)$, which puts the system (1.1) into the explicit fast–slow form

$$\begin{aligned} x' &= f(x, y, \varepsilon), & x &\in \mathbf{R}^{N_s}, \\ \varepsilon y' &= g(x, y, \varepsilon), & y &\in \mathbf{R}^{N_f}. \end{aligned} \quad (1.5)$$

We emphasize that, in general, we have no knowledge whatsoever of the transformation that puts system (1.1) into an explicit fast–slow form. Here, f and g are smooth functions of their arguments, the manifold \mathcal{L} is transformed smoothly, and $\det(D_y g)_0(z) \equiv \det(D_y g(z, 0)) \neq 0$ on the manifold $\mathcal{L}_{[0]} = \{z | g(z, 0) = 0\}$ (on which the dynamics reduce for $\varepsilon = 0$), see also [4].

Due to the above assumption, it turns out to be natural to split the analysis of the accuracy and convergence of the functional iteration into two parts. In the first part, which we present in this article, we work directly on systems that are already in explicit fast–slow form (1.5). In the context of these systems, the accuracy and convergence analysis may be carried out completely in terms of the small parameter ε . The system geometry – the slow manifold and the fast fibers transverse to \mathcal{L} – makes the convergence analysis especially transparent. Then, in the second part, we work with the more general systems (1.1). For these, the accuracy analysis proceeds along similar lines as that for this first part, with the same type of result as Theorem 2.1 below. However, the convergence analysis is considerably more involved than that for explicit fast–slow systems. For these general systems, one must analyze a series of different scenarios depending on the relative orientations of (i) the tangent space to \mathcal{L} , (ii) the tangent spaces to the fast fibers at their base points on \mathcal{L} , and (iii) the hyperplane of the observables u . Moreover, all of the analysis must be carried out through the lens of the coordinate change (1.4) and its inverse, so that it is less transparent than it is in part one. Part two will be presented as a subsequent article.

As applied specifically to explicit fast–slow systems (1.5), the m –th iterative algorithm (1.3) is based on the $(m + 1)$ –st derivative condition,

$$\left(\frac{d^{m+1}y}{dt^{m+1}} \right) (x_0, y) = 0. \quad (1.6)$$

In particular, for each m and for any arbitrary, but fixed, value of the observable $x_0 \in K$, one makes an initial guess for $h(x_0)$ and uses the m –th iterative algorithm

to approximate the appropriate zero of this $(m + 1)$ -st derivative, where the end (*converged*) result of the iteration is the improved approximation of $h(x_0)$.

For each $m = 0, 1, \dots$, the m -th iterative algorithm is defined by the map $F_m : \mathbf{R}^{N_f} \rightarrow \mathbf{R}^{N_f}$,

$$F_m(y) = y - (-H)^{m+1} \left(\frac{d^{m+1}y}{dt^{m+1}} \right) (x_0, y), \quad (1.7)$$

where H is an arbitrary positive number whose magnitude is $\mathcal{O}(\varepsilon)$ for stability reasons. We seed with some value $y^{(1)}$ and generate the sequence

$$\{y^{(r+1)} \equiv F_m(y^{(r)}) \mid r = 1, 2, \dots\}. \quad (1.8)$$

Here also, one prescribes a tolerance TOL_m and terminates the iteration procedure when $\|y^{(r+1)} - y^{(r)}\| < \text{TOL}_m$ for some $r \geq 1$. The output of this m -th algorithm is the last member of the sequence $\{y^{(r+1)}\}$, denoted by $y_m^\#$.

1.3 Statement of the main results

In this article, we first examine the m -th iterative algorithm in which an analytical formula for the $(m + 1)$ -st derivative is used, and we prove that it has a fixed point $y = h_m(x_0)$, which is $\mathcal{O}(\varepsilon^{m+1})$ close to the corresponding point $h(x_0)$ on the invariant manifold \mathcal{L} , for each $m = 0, 1, \dots$. See Theorem 2.1 below.

Second, we determine the conditions on $(D_y g)_0$ under which the m -th iterative algorithm converges to this fixed point, again with an analytical formula for the $(m + 1)$ -st derivative. In particular, for $m = 0$, the iteration converges for all systems (1.5) for which $(D_y g)_0$ is uniformly Hurwitz on $\mathcal{L}_{[0]}$ and provided that the iterative step size H is small enough. For each $m \geq 1$, convergence of the algorithm imposes more stringent conditions on H and on the spectrum of $(D_y g)_0$. In particular, if $\sigma((D_y g)_0)$ is contained in certain sets in the complex plane, which we identify completely, then the iteration converges for small enough values of the iterative step size H , see Theorem 3.1. These sets do not cover the entire half-plane, and thus complex eigenvalues can, in general, make the algorithm divergent.

Third, we show explicitly how the Recursive Projection Method (RPM) of Shroff and Keller [15] stabilizes the functional iteration for each $m \geq 1$ in those regimes where the iteration is unstable. This stabilization result is useful for practical implementation in the equation-free context; and, the RPM may also be used to accelerate convergence in those regimes in which the iterations converge slowly. Alternatively, the Newton–Krylov Generalized Minimal Residual Method (NK-GMRES [9]) may be used to achieve this stabilization.

Fourth, we analyze the influence of the tolerance, or stopping criterion, used to terminate the functional iteration. We show that, when the tolerance TOL_m for the m -th algorithm is set to $\mathcal{O}(\varepsilon^{m+1})$, the output $y_m^\#$ also satisfies the asymptotic estimate $\|y_m^\# - h(x_0)\| = \mathcal{O}(\varepsilon^{m+1})$.

Finally, we extend the accuracy and convergence analyses to the case where a forward difference approximation of the $(m+1)$ -st derivative is used in the iteration, instead of the analytical formula. As to the accuracy, we find that the m -th iterative algorithm also has a fixed point $y = \hat{h}_m(x_0)$ which is $\mathcal{O}(\varepsilon^{m+1})$ close to $h(x_0)$, so that the iteration in this case is as accurate asymptotically as the iteration with the analytical formula. Then, as to the stability, we find that the m -th iterative algorithm with a forward difference approximation of the $(m+1)$ -st derivative converges unconditionally for $m = 0$. Moreover, for $m = 1, 2, \dots$, the convergence is for a continuum of values of the iterative step size H and without further restrictions on $(D_y g)_0$, other than that it is uniformly Hurwitz on $\mathcal{L}_{[0]}$, see Theorem 6.1. These advantages stem from the use of a forward difference approximation, and we will show in a future work that the use of implicitly defined maps F_m yields similar advantages.

Throughout this article, we shall refer to some basic facts about the N_s -dimensional, slow, invariant, and normally attracting manifold \mathcal{L} . As stated above, \mathcal{L} is the graph of a function h ,

$$\mathcal{L} = \{(x, y) \mid x \in K, y = h(x)\}, \quad (1.9)$$

for some set K . Here, the function $h : K \rightarrow \mathbf{R}^{N_f}$ satisfies the invariance equation

$$g(x, h(x), \varepsilon) - \varepsilon Dh(x)f(x, h(x), \varepsilon) = 0, \quad (1.10)$$

and it is $\mathcal{O}(\varepsilon)$ close to the critical manifold, which is the graph of $h_0(x)$, uniformly for $x \in K$.

It is insightful to recast this invariance equation in the form

$$(-Dh(x), I_{N_f}) G(x, h(x), \varepsilon) = 0, \quad \text{where} \quad G \equiv \begin{pmatrix} \varepsilon f \\ g \end{pmatrix}, \quad (1.11)$$

which reveals a clear geometric interpretation. Since \mathcal{L} corresponds to the zero level set of the function $-h(x) + y$ by Eq. (1.9), the rows of the $N_f \times N$ gradient matrix $(-Dh(x), I_{N_f})$ form a basis for $N_z \mathcal{L}$, the space normal to the slow manifold at the point $z = (x, h(x)) \in \mathcal{L}$. Thus, Eq. (1.11) states that the vector field G is perpendicular to this space and hence contained in the space tangent to the slow manifold, $T_z \mathcal{L}$.

2 Existence of a fixed point $h_m(x_0)$ and its proximity to $h(x_0)$

We rewrite the map F_m , given in Eq. (1.7), as

$$F_m(y) = y - L_m(x_0, y), \quad (2.1)$$

where the function $L_m : \mathbf{R}^N \rightarrow \mathbf{R}^{N_f}$ is given by

$$L_m(z) \equiv (-H)^{m+1} \left(\frac{d^{m+1}y}{dt^{m+1}} \right) (z), \quad \text{for any } m = 0, 1, \dots, \quad (2.2)$$

where $z = (x_0, y)$. The fixed points, $y = h_m(x_0)$, of F_m are determined by the equation

$$L_m(x_0, h_m(x_0)) = 0,$$

that is, by the $(m + 1)$ -st derivative condition (1.6). The desired results on the existence of the fixed point $h_m(x_0)$ and on its proximity to $h(x_0)$ are then immediately at hand from the following theorem:

Theorem 2.1 *For each $m = 0, 1, \dots$, the $(m + 1)$ -st derivative condition (1.6),*

$$L_m(x, y) \equiv (-H)^{m+1} \left(\frac{d^{m+1}y}{dt^{m+1}} \right) (x, y) = 0, \quad (2.3)$$

can be solved for y to yield an N_s -dimensional manifold \mathcal{L}_m which is the graph of a function $h_m : K \rightarrow \mathbf{R}^{N_f}$ over x . Moreover, the asymptotic expansions of h_m and h agree up to and including terms of $\mathcal{O}(\varepsilon^m)$,

$$h_m(\cdot) = \sum_{i=0} \varepsilon^i h_{m,i}(\cdot) = \sum_{i=1}^m \varepsilon^i h_{[i]}(\cdot) + \mathcal{O}(\varepsilon^{m+1}).$$

This theorem guarantees that, for each $x_0 \in K$, there exists an isolated fixed point $y = h_m(x_0)$ of the functional iteration algorithm. Moreover, this fixed point varies smoothly with x_0 , and the approximation $(x_0, h_m(x_0))$ of the point $(x_0, h(x_0))$ on the actual invariant slow manifold is valid up to $\mathcal{O}(\varepsilon^{m+1})$.

The remainder of this section is devoted to the proof of this theorem. We prove it for $m = 0$ and $m = 1$ in Sections 2.1 and 2.2, respectively. Then, in Section 2.3, we use induction to prove the theorem for general m .

2.1 Proof of Theorem 2.1 for $m = 0$

We show, for each $x \in K$, that $L_0(z)$ has a root $y = h_0(x)$, that h_0 lies $\mathcal{O}(\varepsilon)$ close to $h_{[0]}(x)$, the corresponding point on the critical manifold, and that the graph of the function h_0 over K forms a manifold.

For $m = 0$, definition (2.2), the chain rule, and the ODEs (1.5) yield

$$L_0 = -Hy' = -\varepsilon^{-1}Hg. \quad (2.4)$$

Substituting the asymptotic expansion $y = h_0(x) = \sum_{i=0} \varepsilon^i h_{0,i}(x)$ into this formula and combining it with the condition $L_0 = 0$, we find that, to leading order,

$$g(x, h_{0,0}(x), 0) = 0,$$

where we have removed the $\mathcal{O}(1)$, nonzero, scalar quantity $-H/\varepsilon$. In comparison, the invariance equation (1.10) yields

$$g(x, h_{[0]}(x), 0) = 0, \quad (2.5)$$

to leading order, see Eq. (A.2) in Appendix A. Thus $h_{0,0}$ can be chosen to be equal to $h_{[0]}$, and $L_0(z)$ has a root that is $\mathcal{O}(\varepsilon)$ -close to $y = h(x)$.

It remains to show that the graph of the function h_0 is an N_s -dimensional manifold \mathcal{L}_0 . Using Eq. (2.4), we calculate

$$(D_y L_0) = -\varepsilon^{-1}H(D_y g),$$

where all quantities are evaluated at $(x, h_0(x), \varepsilon)$. Moreover,

$$(D_y L_0)(x, h_0(x)) = -\varepsilon^{-1}H(D_y g)_0 + \mathcal{O}(\varepsilon),$$

with $(\cdot)_0 = (\cdot)(x, h_{0,0}(x), 0) = (\cdot)(x, h_{[0]}(x), 0)$, since $h_{0,0} = h_{[0]}$. Thus, the Jacobian $(D_y L_0)(x, h_0(x))$ is non-singular for $0 < \varepsilon \ll 1$, because $H = \mathcal{O}(\varepsilon)$ by assumption and because $\det(D_y g)_0 \neq 0$, see the Introduction. Therefore, we have

$$\det(D_y L_0)(x, h_0(x)) \neq 0, \quad \text{for all } x \in K,$$

and hence \mathcal{L}_0 is a manifold by the Implicit Function Theorem and [14, Theorem 1.13]. This completes the proof of the theorem for the case $m = 0$.

2.2 The proof of Theorem 2.1 for $m = 1$

In this section, we treat the $m = 1$ case. Technically speaking, one may proceed directly from the $m = 0$ case to the induction step for general m . Nevertheless, we

find it useful to present a concrete instance and a preview of the general case, and hence we give a brief analysis of the $m = 1$ case here.

We calculate

$$L_1 = (-H)^2 y'' = -H(-Hy')' = -HL'_0 = -\varepsilon^{-1}H(D_z L_0)G.$$

Using the ODEs (1.5) and Eq. (2.4), we rewrite this as

$$L_1 = (-\varepsilon^{-1}H)^2 [\varepsilon(D_x g)f + (D_y g)g]. \quad (2.6)$$

We recall that the solution is denoted by $y = h_1(x)$ and that we write its asymptotic expansion as $h_1(x) = \sum_{i=0} \varepsilon^i h_{1,i}(x)$. Substituting this expansion into Eq. (2.6) and recalling that $H = \mathcal{O}(\varepsilon)$, we obtain at $\mathcal{O}(1)$

$$L_1 = (-\varepsilon^{-1}H)^2 (D_y g)_0 g_0 + \mathcal{O}(\varepsilon),$$

where $(\cdot)_0 = (\cdot)(x, h_{1,0}(x), 0)$. Hence, $y = h_{[0]}(x)$ is a root of L_1 to leading order by Eq. (2.5) and $\det(D_y g)_0 \neq 0$, and therefore $h_{1,0}$ can be selected to be equal to $h_{[0]}$.

At $\mathcal{O}(\varepsilon)$, we obtain

$$(-\varepsilon^{-1}H)^2 (D_y g)_0 [(D_y g)_0^{-1} (D_x g)_0 f_0 + (D_y g)_0 h_{1,1} + (D_\varepsilon g)_0] = 0, \quad (2.7)$$

where we used the expansion

$$g(x, h_1, \varepsilon) = g_0 + \varepsilon [(D_y g)_0 h_{1,1} + (D_\varepsilon g)_0] + \mathcal{O}(\varepsilon^2)$$

and that $g_0 = g(x, h_{1,0}, 0) = g(x, h_{[0]}, 0)$. Differentiating both members of the identity $g(x, h_{[0]}(x), 0) = 0$ with respect to x , we obtain

$$(D_x g)_0 + (D_y g)_0 (Dh_{[0]}) = 0,$$

whence $(D_y g)_0^{-1} (D_x g)_0 = -Dh_{[0]}$. Removing the invertible prefactor $(-H/\varepsilon)^2 (D_y g)_0$, we find that Eq. (2.7) becomes

$$-(Dh_{[0]})f_0 + (D_y g)_0 h_{1,1} + (D_\varepsilon g)_0 = 0.$$

This equation is identical to Eq. (A.3) in Appendix A, and thus $h_{1,1} = h_{[1]}$. Hence, we have shown that the asymptotic expansion of $h_1(x)$ agrees with that of $h(x)$ up to and including terms of $\mathcal{O}(\varepsilon)$, as claimed for $m = 1$.

Finally, the graph of the function h_1 forms an N_s -dimensional manifold \mathcal{L}_1 . This may be shown in a manner similar to that used above for \mathcal{L}_0 in the case $m = 0$. This completes the proof for $m = 1$.

2.3 The induction step: the proof of Theorem 2.1 for general m

In this section, we prove the induction step that establishes Theorem 2.1 for all m . We assume that the conclusion of Theorem 2.1 is true for m and show that it also holds for $m + 1$, *i.e.*, that the condition

$$[(D_z L_m)(x, y)] G(x, y, \varepsilon) = 0 \quad (2.8)$$

can be solved for y to yield $y = h_{m+1}(x)$, where

$$h_{m+1}(\cdot) = \sum_{i=0}^{m+1} \varepsilon^i h_{[i]}(\cdot) + \mathcal{O}(\varepsilon^{m+2}).$$

To begin with, we recast the $(m + 1)$ -st derivative condition Eq. (2.3) in a form that is reminiscent of the invariance equation, Eq. (1.11). Let $m \geq 0$ be arbitrary but fixed. It follows from definition (2.2), Eq. (1.11), and Eq. (1.5) that

$$L_m = -H \frac{d}{dt} \left((-H)^m \frac{d^m y}{dt^m} \right) = -H \frac{dL_{m-1}}{dt} = -\varepsilon^{-1} H (D_z L_{m-1}) G. \quad (2.9)$$

Therefore, the $(m + 1)$ -st derivative condition (2.3) can be rewritten in the desired form as

$$(D_z L_{m-1}) G = 0, \quad (2.10)$$

where we have removed the $\mathcal{O}(1)$, nonzero, scalar quantity $-H/\varepsilon$.

The induction step will now be established using a bootstrapping approach. First, we consider a modified version of Eq. (2.8), namely the condition

$$[(D_z L_m)(x, h_m(x))] G(x, y, \varepsilon) = 0, \quad (2.11)$$

in which the matrix $D_z L_m$ is evaluated on \mathcal{L}_m (already determined at the m -th iteration) instead of on the as-yet unknown \mathcal{L}_{m+1} . This equation is easier to solve for the unknown y , since y appears only in G . We now show that the solution $y = \tilde{h}_{m+1}(x)$ of this condition approximates h up to and including $\mathcal{O}(\varepsilon^{m+1})$ terms.

Lemma 2.1 *The condition Eq. (2.11) can be solved for y to yield*

$$y = \tilde{h}_{m+1}(x) = \sum_{i=0}^{m+1} \varepsilon^i h_{[i]}(x) + \mathcal{O}(\varepsilon^{m+2}), \quad \text{for all } x \in K. \quad (2.12)$$

Then, with this first lemma in hand, we bootstrap up from the solution $y = \tilde{h}_{m+1}$ of this modified condition to find the solution $y = h_{m+1}$ of the full $(m + 1)$ -st derivative condition, Eq. (2.10). Specifically, we show that their asymptotic expansions agree up to and including terms of $\mathcal{O}(\varepsilon^{m+1})$,

Lemma 2.2 *The condition (2.8), can be solved for y to yield*

$$y = h_{m+1}(x) = \sum_{i=0}^{m+1} \varepsilon^i \tilde{h}_{m+1,i}(x) + \mathcal{O}(\varepsilon^{m+2}), \quad \text{for all } x \in K.$$

Given these lemmata – the proofs of which are given in appendix B – Theorem 2.1 follows directly.

3 Stability analysis of the fixed point $h_m(x_0)$

In this section, we analyze the stability type of the fixed point $y = h_m(x_0)$ of the functional iteration scheme given by $F_m(y)$. To fix the notation, we let

$$\sigma(D_y g)_0 = \{ \lambda_\ell = \lambda_{\ell,R} + i \lambda_{\ell,I} = |\lambda_\ell| e^{i\theta_\ell} = \lambda_{\ell,R}(1 + i \tan\theta_\ell) : \ell = 1, \dots, N_f \} \quad (3.1)$$

and remark that normal attractivity of the slow manifold implies that $\lambda_{\ell,R} < 0$ (equivalently, $\pi/2 < \theta_\ell < 3\pi/2$) for all $\ell = 1, \dots, N_f$. Then, we prove the following theorem:

Theorem 3.1 *For each $m = 0, 1, \dots$, the functional iteration scheme defined by F_m is stable if and only if the following two conditions are satisfied for all $\ell = 1, \dots, N_f$:*

$$\theta_\ell \in \mathcal{S}_m \equiv \bigcup_{k=0, \dots, m} \left(\frac{2m + 4k + 1}{2(m+1)}\pi, \frac{2m + 4k + 3}{2(m+1)}\pi \right) \cap \left[\left(\frac{\pi}{2}, \frac{3\pi}{2} \right) \bmod 2\pi \right] \quad (3.2)$$

and

$$0 < H < H_\ell^{\max} \equiv \frac{\varepsilon}{|\lambda_\ell|} [2 \cos((m+1)(\theta_\ell - \pi))]^{1/(m+1)}. \quad (3.3)$$

In particular, if $\lambda_1, \dots, \lambda_{N_f}$ are real, then the functional iteration is stable for all H satisfying

$$H < H^{\max} \equiv 2^{1/(m+1)} \frac{\varepsilon}{\|D_y g\|_2}. \quad (3.4)$$

The graphs of the stability regions for $m = 0, 1, 2, 3$ are given in Figure 1.

We now prove this theorem. By definition, $h_m(x_0)$ is exponentially attracting if and only if

$$\sigma((DF_m)(h_m(x_0))) \subset B(0; 1), \quad (3.5)$$

where $B(0; 1)$ denotes the open ball of radius one centered at the origin. To determine the spectrum of $(DF_m)(h_m(x_0))$, we use Eq. (2.1) and Lemma B.1 to obtain

$$\begin{aligned} (DF_m)(y) &= I_{N_f} - (D_y L_m)(x_0, y) \\ &= I_{N_f} - \left(-\varepsilon^{-1} H(D_y g)(x_0, y, 0)\right)^{m+1} + \mathcal{O}(\varepsilon, \|g_0(x_0, y)\|). \end{aligned}$$

Letting $y = h_m(x_0)$ in this expression and observing that $\|g_0(x_0, h_m(x_0))\| = \mathcal{O}(\varepsilon)$ by virtue of the estimate $h_m = h_0 + \mathcal{O}(\varepsilon)$ (see Theorem 2.1) and Eq. (2.5), we obtain to leading order

$$(DF_m)(h_m(x_0)) = I_{N_f} - \left(-\varepsilon^{-1} H D_y g\right)_0^{m+1}, \quad (3.6)$$

where $z_m = (x_0, h_m(x_0))$ and the notation $(\cdot)_0$ signifies that the quantity in parentheses is evaluated at the point $(x_0, h_{[0]}(x_0)) \in \mathcal{L}_{[0]}$. Finally, then, we find to leading order

$$\sigma((DF_m)(h_m(x_0))) = \left\{ \mu_\ell = 1 - \left(|\lambda_\ell| \varepsilon^{-1} H\right)^{m+1} e^{i(m+1)(\theta_\ell - \pi)} \mid \ell = 1, \dots, N_f \right\}. \quad (3.7)$$

In view of Eq. (3.7), condition (3.5) becomes

$$\left| 1 - \left(|\lambda_\ell| \varepsilon^{-1} H\right)^{m+1} e^{i(m+1)(\theta_\ell - \pi)} \right| < 1, \quad \text{for all } \ell = 1, \dots, N_f. \quad (3.8)$$

Here, we note that higher order terms omitted from formula (3.7) do not affect stability for small enough values of ε , because the stability region $B(0; 1)$ is an open set. Next, we study the circumstances in which this stability condition is satisfied. This study naturally splits into the following two cases:

Case 1: The eigenvalues $\lambda_1, \dots, \lambda_{N_f}$ are real. This is the case, for example, when the fast part of system (1.5) corresponds to a spatial discretization of a self-adjoint operator. Here, $\theta_\ell = \pi$ for all ℓ , and thus condition (3.8) reduces to

$$0 < \left(|\lambda_\ell| \varepsilon^{-1} H\right)^{m+1} < 2, \quad \text{for all } \ell = 1, \dots, N_f,$$

which further yields Eq. (3.4).

Case 2: Some of the eigenvalues $\lambda_1, \dots, \lambda_{N_f}$ have nonzero imaginary parts. Using Eq. (3.7), we calculate

$$|\mu_\ell|^2 = 1 + \left(|\lambda_\ell| \varepsilon^{-1} H\right)^{m+1} \left[\left(|\lambda_\ell| \varepsilon^{-1} H\right)^{m+1} - 2 \cos((m+1)(\theta_\ell - \pi)) \right].$$

This equation shows that $|\mu_\ell|^2$ is a convex quadratic function of H^{m+1} . Convexity implies that, if there exists a solution $H_\ell^{\max} > 0$ to the equation $|\mu_\ell| = 1$, then $|\mu_\ell| < 1$ for all $0 < H < H_\ell^{\max}$. Plainly, $|\mu_\ell| = 1$ implies

$$\left(|\lambda_\ell| \varepsilon^{-1} H_\ell^{\max}\right)^{m+1} - 2 \cos((m+1)(\theta_\ell - \pi)) = 0,$$

which yields condition (3.3). Further, the condition that $H_1^{\max}, \dots, H_{N_f}^{\max}$ be real and positive translates into condition (3.2). This completes the proof of Theorem 3.1.

For later comparison to the results of numerical simulations, it is useful to write formula (3.3) explicitly for the first several values of m . For $m = 0$, formula (3.3) becomes

$$H_\ell^{\max} = -\frac{\varepsilon}{|\lambda_\ell|} 2 \cos \theta_\ell,$$

see Figure 1. We note that $H_\ell^{\max} > 0$ for all $\theta_\ell \in (\pi/2, 3\pi/2)$, and thus the fixed point $h_0(x_0)$ is stable for all $0 < H < H^{\max}$, where $H^{\max} = \min_\ell(H_\ell^{\max})$.

For $m = 1$, formula (3.3) becomes

$$H_\ell^{\max} = \frac{\varepsilon}{|\lambda_\ell|} \sqrt{2 \cos(2\theta_\ell)},$$

see Figure 1. We see that, on $(\pi/2, 3\pi/2)$, $H_\ell^{\max} > 0$ *only* if θ_ℓ lies in the subinterval $(3\pi/4, 5\pi/4)$. Therefore, the fixed point $h_1(x_0)$ is stable if and only if (i) $\theta_\ell \in (3\pi/4, 5\pi/4)$, for all $\ell = 1, \dots, N_f$, and (ii) $0 < H < H^{\max} = \min_\ell(H_\ell^{\max})$.

For $m = 2$, formula (3.3) becomes

$$H_\ell^{\max} = -\frac{\varepsilon}{|\lambda_\ell|} [2 \cos(3\theta_\ell)]^{1/3},$$

see Figure 1. Here also, $H_\ell^{\max} > 0$ on $(\pi/2, 3\pi/2)$ *only* if θ_ℓ lies in the subinterval $(5\pi/6, 7\pi/6)$. Thus, $h_2(x_0)$ is stable if and only if (i) $\theta_\ell \in (5\pi/6, 7\pi/6)$, for all $\ell = 1, \dots, N_f$, and (ii) $0 < H < H^{\max} = \min_\ell(H_\ell^{\max})$.

For $m = 3$, formula (3.3) becomes

$$H_\ell^{\max} = \frac{\varepsilon}{|\lambda_\ell|} [2 \cos(4\theta_\ell)]^{1/4},$$

see Figure 1. We observe that, on $(\pi/2, 3\pi/2)$, $H_\ell^{\max} > 0$ *only* if θ_ℓ lies in the subdomain $(\pi/2, 5\pi/8) \cup (7\pi/8, 9\pi/8) \cup (11\pi/8, 3\pi/2)$. Therefore, the fixed point $h_3(x_0)$ is stable if and only if (i) $\theta_\ell \in (\pi/2, 5\pi/8) \cup (7\pi/8, 9\pi/8) \cup (11\pi/8, 3\pi/2)$, for all $\ell = 1, \dots, N_f$, and (ii) $0 < H < H^{\max} = \min_\ell(H_\ell^{\max})$.

4 Stabilization of the algorithm using RPM

In the previous section, we saw that, for any $m \geq 1$, the m -th algorithm in our class of algorithms may have a number of eigenvalues that either are unstable or have modulus only slightly less than one. In this section, we demonstrate how the

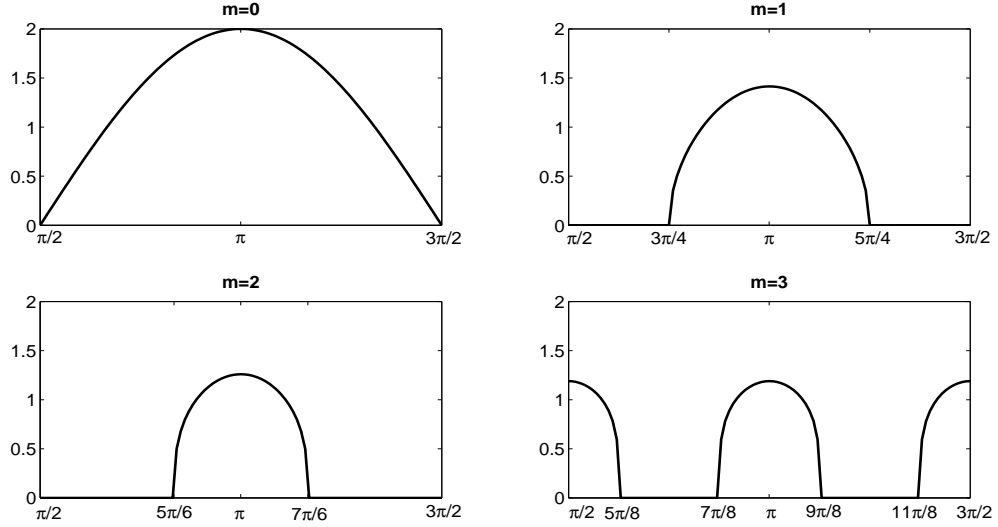


Figure 1: H_ℓ^{max} as a function of $\theta_\ell \in (\pi/2, 3\pi/2)$, for $m = 0, 1, 2, 3$. H_ℓ^{max} is measured in units of $\varepsilon/|\lambda_\ell|$. The eigenvalue μ_ℓ is stable for all $0 < H < H_\ell^{max}$.

Recursive Projection Method (RPM) of Shroff and Keller [15] may be used to stabilize the algorithm or to accelerate its convergence in all such cases.

For the sake of clarity, we assume that $(DF_m)(h_m(x_0))$ has M eigenvalues, labelled $\{\mu_1, \dots, \mu_M\}$, that lie outside the disk $B(0; 1 - \delta)$, for some small, user-specified $\delta > 0$, and that the remaining $N_f - M$ eigenvalues $\{\mu_{M+1}, \dots, \mu_{N_f}\}$ lie inside it. We let \mathbb{P} denote the maximal invariant subspace of $(DF_m)(h_m(x_0))$ corresponding to $\{\mu_1, \dots, \mu_M\}$ and P denote the orthogonal projection operator from \mathbf{R}^{N_f} onto that subspace. Additionally, we use \mathbb{Q} to denote the orthogonal complement of \mathbb{P} in \mathbf{R}^{N_f} and $Q = I_{N_f} - P$ to denote the associated orthogonal projection operator. These definitions induce an orthogonal direct sum decomposition of \mathbf{R}^{N_f} ,

$$\mathbf{R}^{N_f} = \mathbb{P} \oplus \mathbb{Q} = P\mathbf{R}^{N_f} \oplus Q\mathbf{R}^{N_f},$$

and, as a result, each $y \in \mathbf{R}^{N_f}$ has a unique decomposition $y = \tilde{p} + \tilde{q}$, with $\tilde{p} = Py \in \mathbb{P}$ and $\tilde{q} = Qy \in \mathbb{Q}$. The fixed point problem $y = F_m(y)$ may now be written as

$$\tilde{p} = PF_m(\tilde{p} + \tilde{q}), \quad (4.1)$$

$$\tilde{q} = QF_m(\tilde{p} + \tilde{q}). \quad (4.2)$$

The fundamental idea of RPM is to use Newton iteration on Eq. (4.1) and functional iteration on Eq. (4.2). In particular, we decompose the point $y^{(1)}$ (which was

used to generate the sequence $\{y^{(r+1)}\}$ in Eq. (1.8)) via

$$y^{(1)} = \tilde{p}^{(1)} + \tilde{q}^{(1)} = Py^{(1)} + Qy^{(1)}.$$

Then, we apply Newton iteration on Eq. (4.1) (starting with $\tilde{p}^{(1)}$) and functional iteration on Eq. (4.2) (starting with $\tilde{q}^{(1)}$),

$$\begin{aligned}\tilde{p}^{(r+1)} &= \tilde{p}^{(r)} + [I_M - P(DF_m(\tilde{p}^{(r)} + \tilde{q}^{(r)}))P]^{-1} PF_m(\tilde{p}^{(r)} + \tilde{q}^{(r)}), \\ \tilde{q}^{(r+1)} &= QF_m(\tilde{p}^{(r)} + \tilde{q}^{(r)}).\end{aligned}\tag{4.3}$$

The iteration is terminated when $\|y^{(r+1)} - y^{(r)}\| < \text{TOL}_m$, for some $r \geq 1$, as was also the case with functional iteration.

Application of Theorem 3.13 from [15] directly yields that the stabilized (or accelerated) iterative scheme (4.3) converges for all initial guesses $y^{(1)}$ close enough to the fixed point $h_m(x_0)$, as long as

$$1 \notin \sigma(P(DF_m(h_m(x_0)))P) = \{\mu_1, \dots, \mu_M\}.$$

In our case, this condition is satisfied for all $H > 0$, because the fact that \mathcal{L} is normally attracting implies that each eigenvalue λ_ℓ of $D_y g$ is bounded away from zero uniformly over the domain K on which the slow manifold is defined. Thus, the iteration scheme (4.3) converges.

5 Tuning of the tolerance

In this section, we establish that, for every $m = 0, 1, \dots$, $\|y_m^\# - h(x_0)\| = \mathcal{O}(\varepsilon^{m+1})$ whenever $\text{TOL}_m = \mathcal{O}(\varepsilon^{m+1})$. The value returned by the functional iteration is within the tolerance of the point on the true slow manifold for sufficiently small values of the tolerance.

The brunt of the analysis needed to prove this principal result involves showing that, for these small tolerances, $y_m^\#$ is within the tolerance of the fixed point, $h_m(x_0)$. The desired principal result is then immediately obtained by combining this result with the result of Theorem 2.1, where it was shown that $\|h_m(x_0) - h(x_0)\| = \mathcal{O}(\varepsilon^{m+1})$.

We begin by observing that

$$\|y_m^\# - h_m(x_0)\| \leq \|y_m^\# - y^{(r)}\| + \|y^{(r)} - h_m(x_0)\|, \quad \text{for any } r > 0,$$

by the triangle inequality. The first term is $\mathcal{O}(\varepsilon^{m+1})$ by definition, as long as r is chosen large enough so that the stopping criterion, $\|y^{(r+1)} - y^{(r)}\| < \text{TOL}_m$, is satisfied. As to the second term, we may obtain the same type of estimate, as follows: First,

$$y^{(r+1)} - y^{(r)} = F_m(y^{(r)}) - y^{(r)} = -L_m(x_0, y^{(r)}),$$

where we used Eq. (2.1), and hence

$$L_m(x_0, y^{(r)}) = y^{(r)} - y^{(r+1)}.$$

Second, L_m is invertible in a neighborhood of its fixed point, by the Implicit Function Theorem, because the Jacobian of $L_m(x_0, \cdot)$ at $h_m(x_0)$ is

$$(D_y L_m)(z_m) = (-\varepsilon^{-1} H D_y g)_0^{m+1},$$

by Eq. (3.6), and $\det(D_y g) \neq 0$ since $\mathcal{L}_{[0]}$ is normally attracting. Third, by combining these first two observations, we see that

$$y^{(r)} = L_m^{-1}(y^{(r)} - y^{(r+1)}),$$

where L_m^{-1} denotes the local inverse of $L_m(x_0, \cdot)$. Fourth, and finally, by expanding L_m^{-1} around zero, noting that $L_m^{-1}(0) = h_m(x_0)$, and using the triangle inequality, we obtain

$$\|y^{(r)} - h_m(x_0)\| \leq \|(D_y L_m^{-1})(0)\| \|y^{(r)} - y^{(r+1)}\| + \mathcal{O}(\|y^{(r)} - y^{(r+1)}\|^2).$$

Recalling the stopping criterion, we have therefore obtained the desired bound on the second term, as well,

$$\|y^{(r)} - h_m(x_0)\| < \|(D_y L_m^{-1})(0)\| \text{TOL}_m + \mathcal{O}((\text{TOL}_m)^2).$$

Hence, the analysis of this section is complete.

6 The effects of differencing

In a numerical setting, the time derivatives of y are approximated, at each iteration, by a differencing scheme,

$$\left(\frac{d^{m+1}y}{dt^{m+1}}\right)(z) \approx \frac{1}{\hat{H}^{m+1}} (\Delta^{m+1}y)(z), \quad \text{where } z \equiv (x_0, y) \quad \text{and} \quad \hat{H} > 0.$$

In this section, we examine how the approximation and convergence results of Sections 2–5 are affected by the use of differencing. We choose forward differencing,

$$(\Delta^{m+1}y)(z) = \sum_{\ell=0}^{m+1} (-1)^{m+1-\ell} \binom{m+1}{\ell} \phi^y(z; \ell \hat{H}), \quad (6.1)$$

where $\phi(z; t)$ is a (numerically generated) solution with initial condition z , for concreteness of exposition and where \hat{H} is a positive, $\mathcal{O}(\varepsilon)$ quantity. Also, forward differencing is directly implementable in an Equation-Free or legacy code setting.

By the Mean Value Theorem,

$$\begin{aligned} (\Delta^{m+1}y)(z) &= \hat{H}^{m+1} \left(\frac{d^{m+1}y}{dt^{m+1}} \right) (z) + \frac{m+1}{2} \hat{H}^{m+2} \left(\frac{d^{m+2}y}{dt^{m+2}} \right) (\phi(z; \hat{t})) \\ &= \left(-\frac{1}{\eta} \right)^{m+1} \left[L_m(z) - \frac{m+1}{2\eta} L_{m+1}(\phi(z; \hat{t})) \right], \end{aligned} \quad (6.2)$$

where $\eta = H/\hat{H} > 0$ is an $\mathcal{O}(1)$ parameter available for tuning and $\phi(z; \hat{t})$ is the point on the solution $\phi(z; t)$ at some time $\hat{t} \in [0, (m+1)\hat{H}]$. Thus, for the m -th algorithm, the approximation of $d^{m+1}y/dt^{m+1}$ by the above scheme corresponds to generating the sequence $\{y^{(r)} | r = 1, 2, \dots\}$ using the map

$$\hat{F}_m(y) = y - \hat{L}_m(z), \quad z = (x_0, y), \quad (6.3)$$

where

$$\hat{L}_m(z) = (-\eta)^{m+1} (\Delta^{m+1}y)(z) = L_m(z) - \frac{m+1}{2\eta} L_{m+1}(\phi(z; \hat{t})). \quad (6.4)$$

Therefore, by Eq. (6.2),

$$\hat{F}_m(y) = F_m(y) + \frac{m+1}{2\eta} L_{m+1}(\phi(z; \hat{t})).$$

Remark. For convenience in the analysis in this section, we take the flow ϕ to be the exact flow corresponding to Eq. (1.5). The analysis extends directly to many problems for which only a numerical approximation of ϕ is known. For example, if the discretization procedure admits a smooth error expansion (such as exists often for fixed step-size integrators in legacy codes or in the Equation-Free context), then the leading order results still hold, and the map ϕ obtained numerically is sufficiently accurate so that the remainder estimates below hold. In particular, given a p -th order scheme and an integration step size \tilde{h} , it suffices to take $\tilde{h} = \mathcal{O}(\varepsilon)$ to guarantee that the error made in using the numerically-obtained map ϕ is $\mathcal{O}(\varepsilon^p)$. Of course, with other integrators, one could alternatively require that the timestepper be $\mathcal{O}(\varepsilon^{m+2})$ accurate, *i.e.*, of one-higher order of accuracy.

6.1 Existence of a fixed point $\hat{h}_m(x_0)$ of the map \hat{F}_m

In this section, we establish that the map \hat{F}_m has an isolated fixed point $y = \hat{h}_m(x)$ which differs from $h_m(x_0)$ (and thus also from $h(x_0)$, by virtue of Theorem 2.1) only by terms of $\mathcal{O}(\varepsilon^{m+1})$.

The fixed point condition $\hat{F}_m(x_0, y) = y$ may be rewritten as

$$0 = \hat{L}_m(x_0, y) = L_m(x_0, y) - \frac{m+1}{2\eta} L_{m+1}(\phi(x_0, y; \hat{t})), \quad (6.5)$$

where we combined Eqs. (6.3) and (6.4). In order to show that \hat{F}_m has an isolated fixed point $\hat{h}_m(x_0)$ which is $\mathcal{O}(\varepsilon^{m+1})$ -close to $h_m(x_0)$, we need to establish the validity of the following two conditions.

(i) The second term in the right member of Eq. (6.5) satisfies the asymptotic estimate

$$\|L_{m+1}(\phi(z_m; \hat{t}))\| = \mathcal{O}(\varepsilon^{m+1}), \quad \text{where } z_m = (x_0, h_m(x_0)). \quad (6.6)$$

(ii) The Jacobian of \hat{L}_m satisfies

$$\det(D_y \hat{L}_m)(z_m) \neq 0 \quad \text{and} \quad \left\| (D_y \hat{L}_m)(z_m) \right\|_2 = \mathcal{O}(1). \quad (6.7)$$

Let us begin by examining the term $L_{m+1}(\phi(z_m; \hat{t}))$. Let $(\hat{x}, \hat{y}) = \phi(z_m; \hat{t})$. Then, we may write

$$L_{m+1}(\phi(z_m; \hat{t})) = L_{m+1}(\hat{x}, \hat{y}) - L_{m+1}(\hat{x}, h_{m+1}(\hat{x})),$$

because $L_{m+1}(\cdot, h_{m+1}(\cdot)) \equiv 0$ by the definition of L_{m+1} and h_{m+1} . Hence,

$$\|L_{m+1}(\phi(z_m; \hat{t}))\| \leq \|(D_y L_{m+1})(\hat{x}, h_{m+1}(\hat{x}))\| \|\hat{y} - h_{m+1}(\hat{x})\| + \mathcal{O}(\|\hat{y} - h_{m+1}(\hat{x})\|^2). \quad (6.8)$$

Now, $\|(D_y L_{m+1})(\hat{x}, h_{m+1}(\hat{x}))\|$ is $\mathcal{O}(1)$ by Lemma B.1. Next, the triangle inequality yields

$$\|\hat{y} - h_{m+1}(\hat{x})\| \leq \|\hat{y} - h(\hat{x})\| + \|h(\hat{x}) - h_{m+1}(\hat{x})\|.$$

The first term in the right member remains $\mathcal{O}(\varepsilon^{m+1})$ for all times $\hat{t} \in [0, (m+1)\hat{H}]$. Indeed, the initial condition z_m is $\mathcal{O}(\varepsilon^{m+1})$ -close to the normally attracting manifold \mathcal{L} . Thus, the Fenichel normal form [7] guarantees that the orbit generated by this initial condition remains $\mathcal{O}(\varepsilon^{m+1})$ -close to \mathcal{L} for $\mathcal{O}(1)$ time intervals. The second term in the right member is also $\mathcal{O}(\varepsilon^{m+1})$, by Theorem 2.1. Thus, $\|\hat{y} - h_{m+1}(\hat{x})\|$ is also $\mathcal{O}(\varepsilon^{m+1})$. Substituting these estimations into inequality (6.8), we obtain that $\|L_{m+1}(\phi(z_m; \hat{t}))\|$ is $\mathcal{O}(\varepsilon^{m+1})$ and condition (6.6) is satisfied.

Next, we determine the spectrum of $(D_y \hat{L}_m)(z_m)$ to leading order to check condition (6.7). We will work with the definition of $\Delta^{m+1}y$, Eq. (6.1), rather than with formula (6.2) which involves the unknown time \hat{t} . Combining Eqs. (6.1) and (6.3), we obtain

$$\hat{L}_m(z) = \eta^{m+1} \sum_{\ell=0}^{m+1} \binom{m+1}{\ell} (-1)^\ell \phi^y(z; \ell \hat{H}).$$

Differentiating both members of this equation with respect to y , we obtain

$$\left(D_y \hat{L}_m\right)(z) = \eta^{m+1} \sum_{\ell=0}^{m+1} \binom{m+1}{\ell} (-1)^\ell (D_y \phi^y)(z; \ell \hat{H}). \quad (6.9)$$

Next, $(D_y \phi^y)(z_m; t) = e^{(t/\varepsilon)(D_y g)_0}$ to leading order and for all t of $\mathcal{O}(\varepsilon)$ by standard results. Since $\ell \hat{H} = \mathcal{O}(\varepsilon)$ for all $\ell = 0, 1, \dots, (m+1)$, we may use this formula to rewrite Eq. (6.9) to leading order as

$$\left(D_y \hat{L}_m\right)(z_m) = \eta^{m+1} \sum_{\ell=0}^{m+1} \binom{m+1}{\ell} \left(-e^{(\hat{H}/\varepsilon)(D_y g)_0}\right)^\ell = \eta^{m+1} \left(I_{N_f} - e^{(\hat{H}/\varepsilon)(D_y g)_0}\right)^{m+1}.$$

Hence,

$$\sigma\left(\left(D_y \hat{L}_m\right)(z_m)\right) = \left\{ \eta^{m+1} \left(1 - e^{\lambda_\ell \hat{H}/\varepsilon}\right)^{m+1} \middle| \ell = 1, \dots, N_f \right\}, \quad (6.10)$$

where $z_m = (x_0, h_m(x_0))$. This leading order formula for the elements of the spectrum shows that $(D_y \hat{L}_m)(z_m)$ is $\mathcal{O}(1)$ and non-degenerate for all positive $\mathcal{O}(\varepsilon)$ values of H and \hat{H} . Thus, condition (6.7) is also satisfied.

6.2 Stability of the fixed point $\hat{h}_m(x_0)$ for $\eta = 1$

In this section, we determine the stability of the fixed point $\hat{h}_m(x_0)$ under functional iteration using \hat{F}_m in the case that $\hat{H} = H$. Our results for $\hat{H} = H$ are summarized in the following theorem. The general case $\hat{H} \neq H$ is treated in the next section, and the main result there is given in Theorem 6.2.

Theorem 6.1 *Fix $\eta = 1$. The functional iteration scheme defined by \hat{F}_0 is unconditionally stable. For each $m = 1, 2, \dots$, the functional iteration scheme defined by \hat{F}_m is stable if and only if, for each $\ell = 1, \dots, N_f$, the pair (H, θ_ℓ) lies in the stability region the boundary of which is given by the implicit equation*

$$1 = 2 \sum_{j=1}^{m+1} \sum_{k=1}^{j-1} \binom{m+1}{j} \binom{m+1}{k} (-1)^{j+k} e^{-(j+k)H_\ell} \cos((j-k)H_\ell \tan \theta_\ell) + \sum_{k=1}^{m+1} \binom{m+1}{k}^2 e^{-2kH_\ell}, \quad \text{where } H_\ell = -\lambda_{\ell,R} H / \varepsilon > 0. \quad (6.11)$$

Here, the branch of arctan is chosen so that $\theta_\ell \in (\pi/2, 3\pi/2)$. In particular, if $\lambda_1, \dots, \lambda_{N_f}$ are real, then the functional iteration is unconditionally stable. If at least

one of the eigenvalues has a nonzero imaginary part, then a sufficient and uniform (in $\theta_1, \dots, \theta_{N_f}$) condition for stability is that

$$H > \frac{\varepsilon H_s(1)}{\min_\ell |\lambda_{\ell,R}|}, \quad \text{where } H_s(1) = -\ln(2^{1/(m+1)} - 1) \geq 0. \quad (6.12)$$

The stability regions for various values of m are plotted in Figure 3.

Following the procedure used in Section 3, we determine $\sigma((D\hat{F}_m)(\hat{h}_m(x_0)))$ and examine the circumstances in which the stability condition

$$\sigma\left((D\hat{F}_m)(\hat{h}_m(x_0))\right) \subset B(0; 1) \quad (6.13)$$

is satisfied. Equation (6.3) yields

$$(D\hat{F}_m)(\hat{h}_m(x_0)) = I_{N_f} - (D_y \hat{L}_m)(x_0, \hat{h}_m(x_0))$$

and thus also

$$\{\hat{\mu}_\ell\} \equiv \sigma\left((D_y \hat{F}_m)(\hat{h}_m(x_0))\right) = 1 - \sigma\left((D_y \hat{L}_m)(x_0, \hat{h}_m(x_0))\right).$$

Since $\hat{h}_m(x_0)$ differs from $h_m(x_0)$ only at terms of $\mathcal{O}(\varepsilon^{m+1})$, $(D_y \hat{L}_m)(x_0, \hat{h}_m(x_0))$ also differs from $(D_y \hat{L}_m)(x_0, h_m(x_0))$ only at terms of $\mathcal{O}(\varepsilon^{m+1})$. Thus, Eq. (6.10) yields, to leading order and for $\ell = 1, \dots, N_f$,

$$\hat{\mu}_\ell = 1 - (1 - e^{\lambda_\ell H/\varepsilon})^{m+1} = \sum_{k=1}^{m+1} \binom{m+1}{k} (-1)^{k+1} e^{k\lambda_\ell H/\varepsilon}. \quad (6.14)$$

Recalling Eq. (3.1) and defining $H_\ell = -\lambda_{\ell,R} H/\varepsilon$, we rewrite Eq. (6.14) in the form

$$\hat{\mu}_\ell = \sum_{k=1}^{m+1} \binom{m+1}{k} (-1)^{k+1} e^{-kH_\ell(1+i\tan\theta_\ell)}. \quad (6.15)$$

The stability condition (6.13) becomes, then,

$$|\hat{\mu}_\ell| = \left| \sum_{k=1}^{m+1} \binom{m+1}{k} (-1)^{k+1} e^{-kH_\ell(1+i\tan\theta_\ell)} \right| < 1, \quad \text{for all } \ell = 1, \dots, N_f. \quad (6.16)$$

As in Section 3, we distinguish two cases.

Case 1: All of the eigenvalues of $(D_y g)_0$ are real. Then, $\theta_\ell = \pi$ for all $\ell = 1, \dots, N_f$, and hence Eq. (6.15) becomes

$$\hat{\mu}_\ell = \sum_{k=1}^{m+1} \binom{m+1}{k} (-1)^{k+1} e^{-kH_\ell} = 1 - (1 - e^{-H_\ell})^{m+1}.$$

Thus, the spectrum of $(D_y \hat{F}_m)(\hat{h}_m(x_0))$ is contained in $(0, 1)$ for all positive $\mathcal{O}(\varepsilon)$ values of H . Equivalently, the fixed point $\hat{h}_m(x_0)$ is *unconditionally stable* for these values of H .

These results may be interpreted both in the context of the m -th iterative algorithm for each fixed m , as well as in the context of using the algorithms as an integrated class. In particular, for each fixed m , the rate of convergence to the fixed point of the m -th algorithm increases as H increases. Also, for any fixed iterative step size H , the rate of convergence of the m -th algorithm to its fixed point decreases as the order, m , of the iterative algorithm increases. This information is important for determining how large an m one should use, especially when using the algorithms as an integrated class.

Case 2: Some of the eigenvalues of $(D_y g)_0$ have nonzero imaginary parts. When this is the case, some of the eigenvalues may be unstable for certain values of H . Figure 2 demonstrates this: in it, we have drawn the complex eigenvalue $\hat{\mu}_\ell$ for various values of H and for $m = 0, 1, 2, 3$. Plainly, $\hat{\mu}_\ell$ is unstable for $m > 0$ and for H small enough, as $|\hat{\mu}_\ell| > 1$. We determine the stability regions in the (θ_ℓ, H_ℓ) -plane as functions of m .

First, we derive the uniform bound (6.12). Using formula (6.15), we calculate

$$|\hat{\mu}_\ell| \leq \sum_{k=1}^{m+1} \binom{m+1}{k} e^{-kH_\ell} = (1 + e^{-H_\ell})^{m+1} - 1, \quad (6.17)$$

and thus $|\hat{\mu}_\ell| < 1$, for all $H_\ell > H_s(1)$. Recalling that $H_\ell = -\lambda_{\ell,R}H/\varepsilon$, we conclude that all of the eigenvalues $\hat{\mu}_\ell$ lie in the unit disk (equivalently, the m -th algorithm is stable) for all $\mathcal{O}(\varepsilon)$ values of H greater than $\varepsilon H_s(1)/\min_\ell |\lambda_{\ell,R}|$, irrespective of the values of $\theta_1, \dots, \theta_{N_f}$. This is demonstrated in Figure 3.

Next, we derive formulae which describe exactly the stability regions. For $m = 0$, Eq. (6.12) yields $H_s(1) = 0$. Thus, $|\hat{\mu}_\ell| < 1$ for all positive $\mathcal{O}(\varepsilon)$ values of H and for all $\ell = 1, \dots, N_f$. As a result, the fixed point $\hat{h}_0(x_0)$ is *unconditionally stable* for positive, $\mathcal{O}(\varepsilon)$ values of H , see also Figure 3.

For $m = 1$, Eq. (6.15) becomes

$$\hat{\mu}_\ell = 2e^{-H_\ell(1+i \tan \theta_\ell)} - e^{-2H_\ell(1+i \tan \theta_\ell)}.$$

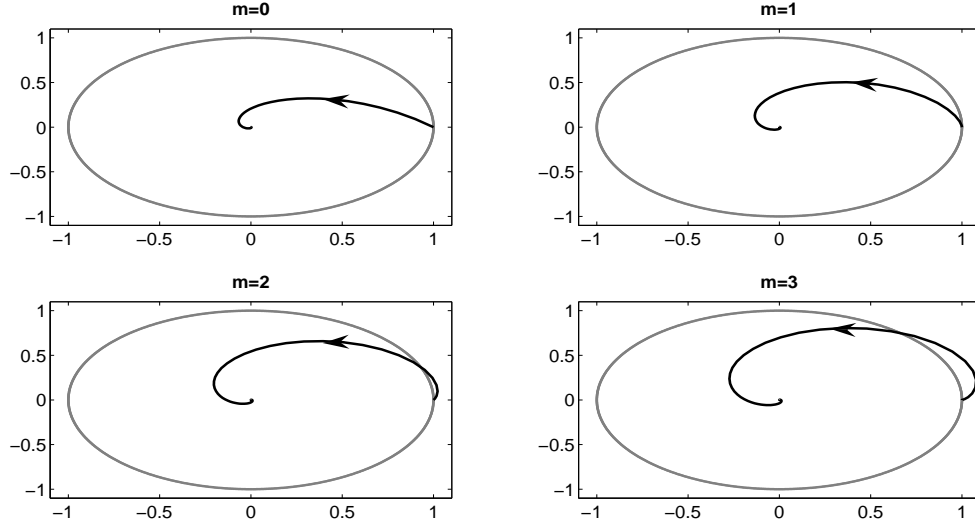


Figure 2: The eigenvalue $\hat{\mu}_\ell$ for values of H between zero and 100ε . The thick line denotes the boundary of the stability region (*i.e.*, the unit circle). The eigenvalue λ_ℓ was taken to be $-1 + i$ for each one of the graphs. The arrow points to increasing values of H .

Writing $\overline{\hat{\mu}_\ell}$ for the complex conjugate of $\hat{\mu}_\ell$, then, we calculate

$$|\hat{\mu}_\ell|^2 = \hat{\mu}_\ell \overline{\hat{\mu}_\ell} = 4e^{-2H_\ell} - 4e^{-3H_\ell} \cos(H_\ell \tan \theta_\ell) + e^{-4H_\ell}. \quad (6.18)$$

Using this formula, we recast the stability condition (6.16) into the form

$$4e^{-2H_\ell} - 4e^{-3H_\ell} \cos(H_\ell \tan \theta_\ell) + e^{-4H_\ell} < 1.$$

In particular, the boundary of the stability region can be obtained by equating the expression in the left member of this inequality to one and solving for θ_ℓ , to obtain

$$\theta_\ell = \arctan \left(H_\ell^{-1} \left[\arccos \left[\frac{1}{4} e^{-H_\ell} + e^{H_\ell} - \frac{1}{4} e^{3H_\ell} \right] + 2k\pi \right] \right).$$

Here, $k \in \mathbf{Z}$ and the branch of \arctan is chosen so that $\theta_\ell \in (\pi/2, 3\pi/2)$. We have plotted the stability region in Figure 3. We also note here that the boundary of the stability region close to $\pi/2$ and to $3\pi/2$ has fine structure, see Figure 4.

For a general value of m , the stability condition (6.16) is

$$|\hat{\mu}_\ell| = \left| \sum_{k=1}^{m+1} \binom{m+1}{k} (-1)^{k+1} e^{-kH_\ell(1+i \tan \theta_\ell)} \right| < 1, \quad \text{for all } \ell = 1, \dots, N_f.$$

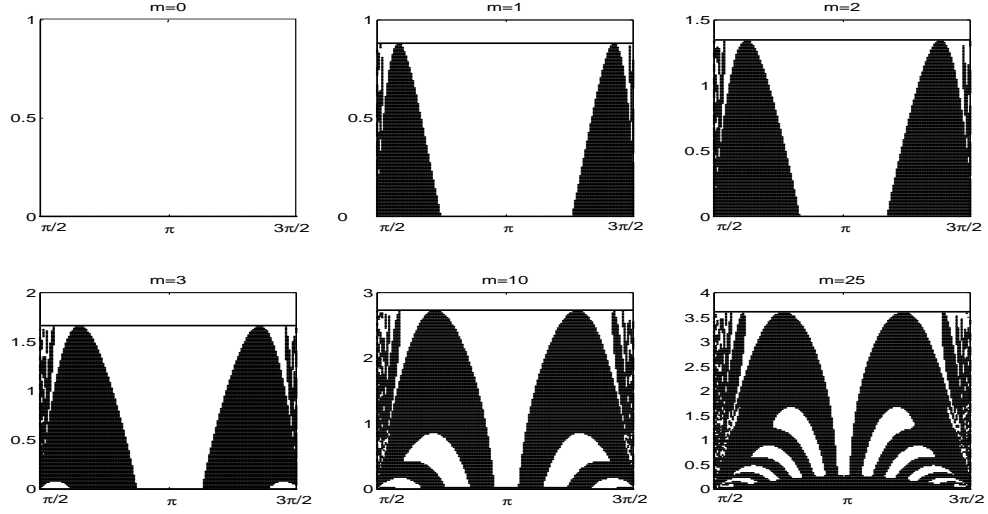


Figure 3: The regions of H for which $|\mu_\ell| < 1$ as functions of $\theta_\ell \in (\pi/2, 3\pi/2)$. White corresponds to stability ($|\mu_\ell| < 1$) and black to instability ($|\mu_\ell| > 1$). H is measured in units of $\varepsilon/|\lambda_{\ell,R}|$. The angle θ_ℓ takes values on $(\pi/2, 3\pi/2)$ and the black horizontal line corresponds to the uniform bound $H_s(1)$ of Eq. (6.12).

Now, using Eq. (6.15), we calculate

$$\begin{aligned}
|\hat{\mu}_\ell|^2 &= \hat{\mu}_\ell \overline{\hat{\mu}_\ell} \\
&= \sum_{j=1}^{m+1} \sum_{k=1}^{m+1} \binom{m+1}{j} \binom{m+1}{k} (-1)^{j+k} e^{-(j+k)H_\ell} e^{i(j-k)H_\ell \tan \theta_\ell} \\
&= 2 \sum_{j=1}^{m+1} \sum_{k=1}^{j-1} \binom{m+1}{j} \binom{m+1}{k} (-1)^{j+k} e^{-(j+k)H_\ell} \cos((j-k)H_\ell \tan \theta_\ell) \\
&\quad + \sum_{k=1}^{m+1} \binom{m+1}{k}^2 e^{-2kH_\ell}.
\end{aligned}$$

Equation (6.11) now follows directly.

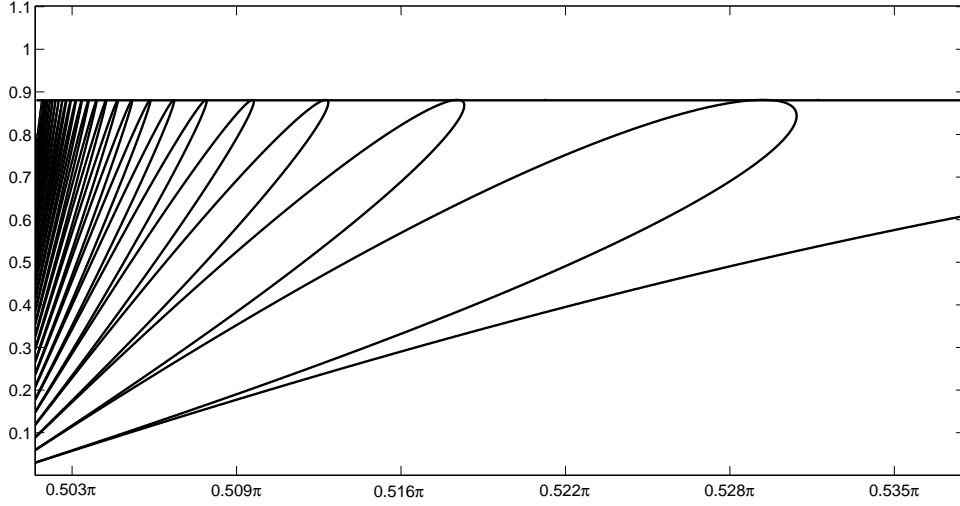


Figure 4: The fine structure of the stability region depicted in Figure 3 (with $m = 1$) close to $\pi/2$. The exterior of the lobes is part of the stability region.

6.3 Stability of the fixed point $\hat{h}_m(x_0)$ for $\eta \neq 1$

In this section, we determine the stability of the fixed point $\hat{h}_m(x_0)$ for $\hat{H} \neq H$. We define the function

$$\hat{H}_m(\eta) = \begin{cases} -\ln(2^{1/(m+1)} - 1), & \text{if } 0 < \eta \leq 1, \\ -\ln|2^{1/(m+1)}/\eta - 1|, & \text{if } \eta > 1. \end{cases} \quad (6.19)$$

Our results are summarized in the following theorem.

Theorem 6.2 *Fix $\eta > 0$. For each $m = 0, 1, 2, \dots$, the functional iteration scheme defined by \hat{F}_m is stable if and only if, for each $\ell = 1, \dots, N_f$, the pair (\hat{H}, θ_ℓ) lies in the stability region the boundary of which is given by the implicit equation*

$$\begin{aligned} 1 &= 2\eta^{2(m+1)} \sum_{j=1}^{m+1} \sum_{k=1}^{j-1} \binom{m+1}{j} \binom{m+1}{k} (-1)^{j+k} e^{-(j+k)\hat{H}_\ell} \cos\left((j-k)\hat{H}_\ell \tan \theta_\ell\right) \\ &+ 2\eta^{m+1} (\eta^{m+1} - 1) \sum_{k=1}^{m+1} \binom{m+1}{k} (-1)^k e^{-k\hat{H}_\ell} \cos\left(k\hat{H}_\ell \tan \theta_\ell\right) \\ &+ \eta^{2(m+1)} \sum_{k=1}^{m+1} \binom{m+1}{k}^2 e^{-2k\hat{H}_\ell} + (\eta^{m+1} - 1)^2, \end{aligned} \quad (6.20)$$

where $\hat{H}_\ell = -\lambda_{\ell,R}\hat{H}/\varepsilon > 0$. Here, the branch of \arctan is chosen so that $\theta_\ell \in (\pi/2, 3\pi/2)$. In particular:

(i) Assume that $\text{Im}(\lambda_\ell) = 0$, for all $\ell = 1, \dots, N_f$. If $0 < \eta < 2^{1/(m+1)}$, then the functional iteration is unconditionally stable. If $\eta > 2^{1/(m+1)}$, then the functional iteration is stable if and only if

$$0 < \hat{H} < \frac{\varepsilon \hat{H}_m(\eta)}{\max_\ell |\lambda_{\ell,R}|}. \quad (6.21)$$

(ii) Assume that at least one of $\text{Im}(\lambda_1), \dots, \text{Im}(\lambda_{N_f})$ is nonzero. If $0 < \eta < 2^{1/(m+1)}$, then a sufficient and uniform (in $\theta_1, \dots, \theta_{N_f}$) condition for stability is

$$\hat{H} > \frac{\varepsilon \hat{H}_m(\eta)}{\min_\ell |\lambda_{\ell,R}|}. \quad (6.22)$$

If $\eta > 2^{1/(m+1)}$, the functional iteration is unstable for any $\theta_1, \dots, \theta_{N_f}$ and for all

$$\hat{H} > \frac{\varepsilon \hat{H}_m(\eta)}{\max_\ell |\lambda_{\ell,R}|}. \quad (6.23)$$

These results are demonstrated in Figures 5 and 6.

As in Section 6.2, we determine when the stability condition (6.13) holds. The analogue of Eqs. (6.14) and (6.15) in this case is, to leading order and for $\ell = 1, \dots, N_f$,

$$\hat{\mu}_\ell = 1 - \eta^{m+1} \left(1 - e^{\lambda_\ell \hat{H}/\varepsilon}\right)^{m+1} = 1 - \eta^{m+1} \left(1 - e^{-\hat{H}_\ell(1+i \tan \theta_\ell)}\right)^{m+1}. \quad (6.24)$$

The stability condition (6.13) becomes, then,

$$|\hat{\mu}_\ell| = \left|1 - \eta^{m+1} \left(1 - e^{-\hat{H}_\ell(1+i \tan \theta_\ell)}\right)^{m+1}\right| < 1, \quad \text{for all } \ell = 1, \dots, N_f. \quad (6.25)$$

Here also, we distinguish two cases.

Case 1: All of the eigenvalues of $(D_y g)_0$ are real. Then, $\theta_\ell = \pi$ for all $\ell = 1, \dots, N_f$, and hence Eq. (6.25) becomes

$$\hat{\mu}_\ell = 1 - \eta^{m+1} (1 - e^{-\hat{H}_\ell})^{m+1}.$$

Plainly, the condition $\hat{\mu}_\ell < 1$ is satisfied for all positive \hat{H}_ℓ and η . Next, solving this equation for η , we obtain an equation for the level curve $\hat{\mu}_\ell = \text{constant}$,

$$\eta = \frac{(1 - \hat{\mu}_\ell)^{1/(m+1)}}{1 - e^{-\hat{H}_\ell}}.$$

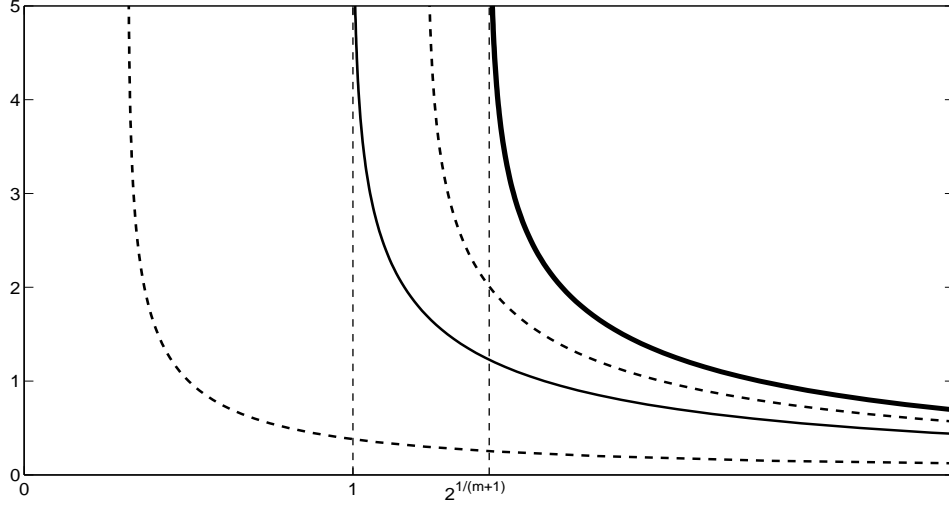


Figure 5: The stability region in the (η, \hat{H}_ℓ) -plane together with the level curves $\hat{\mu}_\ell(\eta, \hat{H}_\ell) = -1$ (thick curve), $\hat{\mu}_\ell(\eta, \hat{H}_\ell) = 0$ (solid curve in the middle), $\hat{\mu}_\ell(\eta, \hat{H}_\ell) = 1$ (union of the two semiaxes). The dashed level curves to the right and left of the level curve $\hat{\mu}_\ell = 0$ correspond to representative positive and negative values of $\hat{\mu}_\ell$, respectively. The eigenvalue $\hat{\mu}_\ell$ is stable for all pairs (η, \hat{H}_ℓ) to the left of the level curve $\hat{\mu}_\ell = -1$.

For $0 < \eta < 2^{1/(m+1)}$ and for all $\mathcal{O}(\varepsilon)$ and positive values of \hat{H} , we obtain $\hat{\mu}_\ell > -1$ (and thus the eigenvalue $\hat{\mu}_\ell$ is stable), see Fig. 5. Therefore, $\sigma((D_y \hat{F}_m)(\hat{h}_m(x_0))) \subset (-1, 1)$, and the fixed point $\hat{h}_m(x_0)$ is *unconditionally stable*.

For $\eta > 2^{1/(m+1)}$, we obtain the condition $0 < \hat{H}_\ell < \hat{H}_m(\eta)$, and Eq. (6.21) follows directly. Finally, we note that, for a fixed value of η and as $\hat{H} \rightarrow \infty$, the spectrum clusters around $1 - \eta^{m+1}$. Thus, the choice $\eta = 1$ is optimal in the sense that large values of \hat{H} bring the spectrum closer to zero.

Case 2: Some of the eigenvalues of $(D_y g)_0$ have nonzero imaginary parts.

In this case, some of the eigenvalues may become unstable for certain combinations of η and \hat{H} , as our analysis in Section 6.2 also showed.

First, we consider the case $0 < \eta < 2^{1/(m+1)}$ and derive the uniform bound (6.22). Using formula (6.24) and working as in Eq. (6.17), we estimate

$$|\hat{\mu}_\ell| \leq |1 - \eta^{m+1}| + \eta^{m+1} \left[(1 + e^{-\hat{H}_\ell})^{m+1} - 1 \right].$$

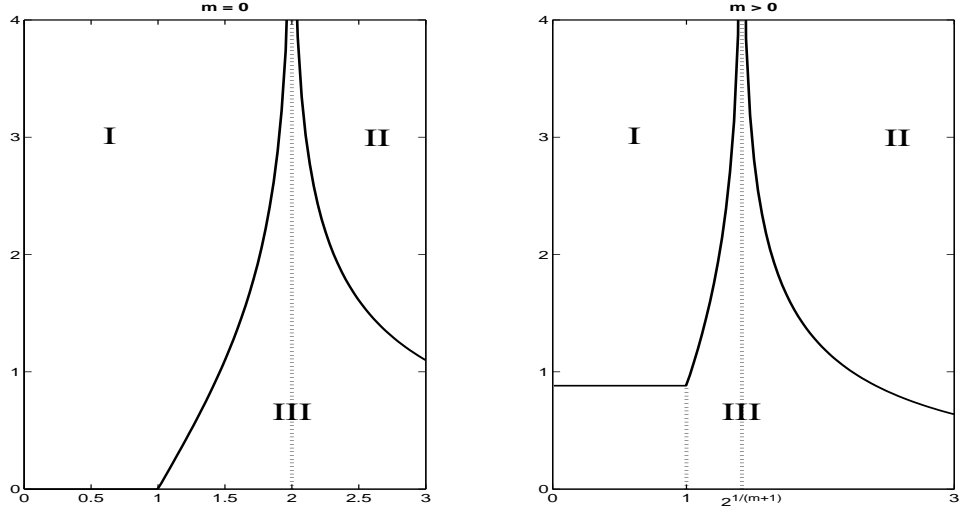


Figure 6: The stability regions in the (η, \hat{H}_ℓ) -plane for $m = 0$ (left panel) and $m = 1, 2, \dots$ (right panel). The eigenvalue $\hat{\mu}_\ell$ is stable in region I, unstable in region II, and its stability type is θ_ℓ -dependent in region III.

Hence

$$|\hat{\mu}_\ell| \leq \begin{cases} 1 + \eta^{m+1} \left[(1 + e^{-\hat{H}_\ell})^{m+1} - 2 \right], & \text{for } 0 < \eta \leq 1, \\ \eta^{m+1} (1 + e^{-\hat{H}_\ell})^{m+1} - 1, & \text{for } \eta > 1. \end{cases}$$

Combining these inequalities with the stability condition $|\hat{\mu}_\ell| < 1$, we obtain the sufficient condition $\hat{H}_\ell > \hat{H}_m(\eta)$, where $\hat{H}_m(\eta)$ is the uniform bound (6.19) (see also Fig. 6). Recalling that $\hat{H}_\ell = -\lambda_{\ell,R} \hat{H} / \varepsilon$, we conclude that, if condition (6.22) is satisfied, then $\sigma((D_y \hat{F}_m)(\hat{h}_m(x_0))) \subset B(0; 1)$, and hence the m -th algorithm is stable.

Next, we consider the case $\eta > 2^{1/(m+1)}$ and derive the uniform bound (6.23). Equation (6.24) yields

$$|1 - \hat{\mu}_\ell| \geq \eta^{m+1} \left(1 - \left| e^{-\hat{H}_\ell} e^{i\hat{H}_\ell \tan \theta_\ell} \right| \right)^{m+1} \geq \eta^{m+1} \left(1 - e^{-\hat{H}_\ell} \right)^{m+1}.$$

Thus, $|1 - \hat{\mu}_\ell| > 2$, for $\eta > 2^{1/(m+1)}$ and $\hat{H}_\ell > \hat{H}_m(\eta)$, and therefore

$$|\hat{\mu}_\ell| \geq ||1 - \hat{\mu}_\ell| - 1| > 1,$$

Hence, $\hat{\mu}_\ell$ is unstable.

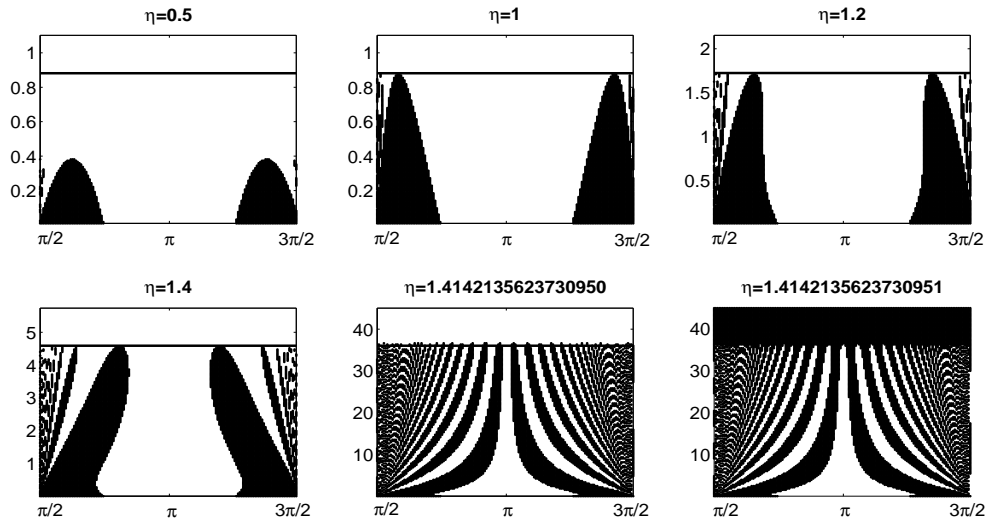


Figure 7: The stability region in the (η, \hat{H}_ℓ) -plane for $m = 1$ and for various values of η . The last two values for η are just below and just above the value $2^{1/(m+1)} = \sqrt{2}$. White denotes stability and black denotes instability.

Remark. Conditions (6.22) and (6.23) may be interpreted by means of the fact that $\sigma((D_y \hat{F}_m)(\hat{h}_m(x_0)))$ clusters around $1 - \eta^{m+1}$ as $\hat{H} \rightarrow \infty$. For $0 < \eta < 2^{1/(m+1)}$, there holds that $-1 < 1 - \eta^{m+1} < 1$. Thus, for \hat{H} large enough, the eigenvalues are contained in the unit disk. On the contrary, $1 - \eta^{m+1} < -1$ for $\eta > 2^{1/(m+1)}$, and thus the eigenvalues lie outside the unit disk for \hat{H} large enough.

Finally, formula (6.20) describing the stability region may be derived in a manner entirely analogous to that used to derive Eq. (6.11).

7 Conclusions and Discussion

In this article, we characterized the accuracy and convergence properties of the class of iterative algorithms introduced in [4] for explicit fast-slow systems (1.5). The m -th member of the class corresponds to a functional iteration scheme to solve the $(m + 1)$ -st derivative condition (1.6). We showed that this condition has an isolated solution, which corresponds to a fixed point of this m -th member and which is accurate up to and including terms of $\mathcal{O}(\varepsilon^m)$, see Theorem 2.1. Also, we derived explicit formulae for the domain of convergence of the functional iteration, both in the case where analytical formulae for the $(m + 1)$ -st derivative are used (see Theorem 3.1)

and in the case where the $(m + 1)$ -st derivatives are estimated through a forward difference scheme (see Theorem 6.1). These convergence results are illustrated in Figures 1, 3, and 4. Further, we demonstrated how the Recursive Projection Method may be used to stabilize the functional iteration in all cases when it is unstable or to accelerate its convergence in those cases where the convergence is slow.

An extension of the analysis presented here to more general multiscale systems (1.1) will be presented in a subsequent article. The analysis of the accuracy of the $(m + 1)$ -st derivative condition presented in Section 2 carries through, essentially (modulo a number of technicalities), in the more general case as well. The analysis of the stability of the functional iteration, on the other hand, is far more involved. The reason for that is that, although the hyperplane $u = u_0$ and the space tangent to the fast fibration over the slow manifold coincide to leading order for explicit fast-slow systems (1.5), this is not the case for the more general systems (1.1). The absence of this feature makes the stability question for the functional iteration far more difficult to answer in the general case.

In addition, we are in the process of generalizing the results of this article to other maps that may be used in the context of the functional iteration scheme developed in [4]. In particular, it is of interest to use maps which are implicitly defined (as opposed to the explicitly defined ones presented in [4] and in this article). Preliminary analytical results for $m = 0$ and $m = 1$ indicate that one may construct functional iteration schemes based on *implicit* maps which not only retain the accuracy of the functional iteration scheme presented in this article but which are also unconditionally stable. Moreover, we think that this analysis may be extended to higher values of m , and we note that it is also possible to carry out the functional iteration with implicitly defined maps even when one only has a legacy code as a timestepper.

A The one-higher-order proposition

In this appendix, we state and prove a technical proposition – called the one-higher-order proposition – about the asymptotic accuracy of approximations of \mathcal{L} given an approximation of the normal space to \mathcal{L} . This result is instrumental in the proof of the technical lemmas contained in the next appendix.

We begin by recalling the useful formulation, Eq. (1.11), of the invariance equation that defines the function $h(x)$, whose graph is the invariant, slow manifold \mathcal{L} . This formulation revealed that the matrix $(-Dh(x), I_{N_f})$ forms a basis for $N_z\mathcal{L}$, the space normal to the slow manifold at the point $z = (x, h(x)) \in \mathcal{L}$.

The function $h(x)$ admits an asymptotic expansion in ε ,

$$h(\cdot) = \sum_{i=0} \varepsilon^i h_{[i]}(\cdot), \quad (\text{A.1})$$

where the coefficients $h_{[i]}$, $i = 0, 1, \dots$, are determined by expanding asymptotically the left member of Eq. (1.10) and setting the coefficient of ε^i equal to zero to obtain

$$g_i - \sum_{\ell=0}^{i-1} (Dh_{[\ell]}) f_{i-1-\ell} = 0, \quad i = 0, 1, \dots,$$

where the sum is understood to be empty for $i = 0$. The first few equations are

$$g_0 = 0, \quad (\text{A.2})$$

$$(D_y g)_0 h_{[1]} + (D_\varepsilon g)_0 - (Dh_{[0]}) f_0 = 0. \quad (\text{A.3})$$

Here, Eq. (A.2) is satisfied identically, Eq. (A.3) yields the coefficient $h_{[1]}$, and so on.

The one-higher-order proposition, which we now state and prove, establishes a connection between the order in ε to which a set N of row vectors approximates $N_z \mathcal{L}$ and the order to which the solution $\eta(x)$ to the condition $NG = 0$ approximates h .

Proposition A.1 *Let $N(x, \varepsilon)$ be an $N_f \times N$ matrix with the property that its rows span $N_z \mathcal{L}$ up to and including terms of $\mathcal{O}(\varepsilon^m)$, for some $m = 0, 1, \dots$. That is, $N(\cdot, \varepsilon)$ is of the form*

$$N(\cdot, \varepsilon) = C \left(- \sum_{i=0}^m \varepsilon^i Dh_{[i]}(\cdot) - \sum_{i \geq m+1} \varepsilon^i R_i(\cdot), I_{N_f} \right), \quad (\text{A.4})$$

where C is a non-singular $N_f \times N_f$ matrix and $R_i \neq Dh_{[i]}$, for $i = m+1, m+2, \dots$, in general. Then, the condition

$$N(x, \varepsilon) G(x, y, \varepsilon) = 0 \quad (\text{A.5})$$

can be solved for y to yield a function $y = \eta(x)$, the asymptotic expansion of which agrees with that of $h(x)$ up to and including terms of $\mathcal{O}(\varepsilon^{m+1})$,

$$\eta(x) = \sum_{i=0} \varepsilon^i \eta_i(x) = \sum_{i=0}^{m+1} \varepsilon^i h_{[i]}(x) + \mathcal{O}(\varepsilon^{m+2}). \quad (\text{A.6})$$

This proposition is called the one-higher-order proposition, because it states that the order to which $\eta(x)$ approximates the full slow manifold is of one higher than that to which N approximates the normal space.

Proof of Proposition A.1. We recall that $h(\cdot) = \sum_{i=0} \varepsilon^i h_{[i]}(\cdot)$, by Eq. (A.1), and that $h_{[i]}$ is determined from the $\mathcal{O}(\varepsilon^i)$ terms of the invariance equation (1.11). Similarly, η_i is determined from the $\mathcal{O}(\varepsilon^i)$ terms of Eq. (A.5). Thus, to establish Eq. (A.6), it suffices to compare the terms of these two equations from $\mathcal{O}(1)$ up through and including $\mathcal{O}(\varepsilon^{m+1})$ and to show that they are equal.

First, for each $i = 0, 1, \dots, m$, the invariance equation (1.11) at $\mathcal{O}(\varepsilon^i)$ is

$$(-Dh_{[0]}, I_{N_f}) G_i + \sum_{\ell=1}^i (-Dh_{[\ell]}, 0) G_{i-\ell} = 0. \quad (\text{A.7})$$

Second, to derive the $\mathcal{O}(\varepsilon^i)$ terms for the condition $NG = 0$, we substitute the hypothesis (A.4) in Eq. (A.5) and left-multiply by C^{-1} to obtain

$$C^{-1} N G = \left(-\sum_{i=0}^m \varepsilon^i Dh_{[i]} + \mathcal{O}(\varepsilon^{m+1}), I_{N_f} \right) G = 0. \quad (\text{A.8})$$

Thus, for each $i = 0, 1, \dots, m$, this condition at $\mathcal{O}(\varepsilon^i)$ is

$$(-Dh_{[0]}, I_{N_f}) G_i + \sum_{\ell=1}^i (-Dh_{[\ell]}, 0) G_{i-\ell} = 0.$$

Plainly, this equation is identical to Eq. (A.7). Thus, $\eta_i = h_{[i]}$, for $i = 0, 1, \dots, m$.

Finally, we look at the $\mathcal{O}(\varepsilon^{m+1})$ terms of the two equations. Eq. (A.7) with $i = m + 1$ is

$$(-Dh_{[0]}, I_{N_f}) G_{m+1} + \sum_{\ell=1}^m (-Dh_{[\ell]}, 0) G_{m+1-\ell} + (-Dh_{[m+1]}, 0) G_0 = 0. \quad (\text{A.9})$$

Also, Eq. (A.8) at $\mathcal{O}(\varepsilon^{m+1})$ is

$$(-Dh_{[0]}, I_{N_f}) G_{m+1} + \sum_{\ell=1}^m (-Dh_{[\ell]}, 0) G_{m+1-\ell} + (R_{m+1}, 0) G_0 = 0. \quad (\text{A.10})$$

We note that $R_{m+1} \neq -Dh_{[m+1]}$, in general. However, $G_0 = 0$, since the terms appearing in Eqs. (A.9)–(A.10) are evaluated at $(x, \eta_0, 0) \equiv (x, h_{[0]}, 0)$. Thus, Eqs. (A.9) and (A.10) also agree, and hence $\eta_{m+1} = h_{[m+1]}$. This completes the proof of the proposition. ■

B Proofs of Lemmata 2.1 and 2.2

In this appendix, we prove lemmata 2.1 and 2.2 characterizing the asymptotic accuracy of the approximation to \mathcal{L} obtained from the $(m + 1)$ -st derivative condition (2.10).

Proof of Lemma 2.1. We write z_m for $(x, h_m(x))$ and z for $(x, h(x))$. The strategy is as follows: We will show that the rows of $(D_z L_m)(z_m, \varepsilon)$ span $N_z \mathcal{L}$ up to and including terms of $\mathcal{O}(\varepsilon^m)$. Then, we will apply Proposition A.1 to establish Eq. (2.12).

The manifold \mathcal{L}_m is the graph of the function h_m , and thus it coincides exactly with the zero level set of the function $-h_m(x) + y$. As a result, the rows of the $N_f \times N$ gradient matrix $(-Dh_m(x), I_{N_f})$ form a basis for $N_{z_m} \mathcal{L}_m$. Second, the function $h_m(\cdot)$ is defined through the $(m + 1)$ -st derivative condition $L_m(\cdot, h_m(\cdot), \varepsilon) = 0$. Therefore, \mathcal{L}_m also coincides with (a connected component of) the zero level set of the function $L_m(z, \varepsilon)$. Thus, the rows of the $N_f \times N$ gradient matrix $(D_z L_m)(x, h_m(x), \varepsilon)$ also form a basis for $N_{z_m} \mathcal{L}_m$. It follows from the existence of these two bases that there exists a non-singular $N_f \times N_f$ matrix C such that

$$(D_z L_m)(\cdot, h_m(\cdot), \varepsilon) = C(-Dh_m(\cdot), I_{N_f}). \quad (\text{B.1})$$

Next, the induction hypothesis implies that the asymptotic expansions of h_m and h agree up to and including terms of $\mathcal{O}(\varepsilon^m)$,

$$h_m(\cdot) = \sum_{i=0}^m \varepsilon^i h_{[i]}(\cdot) + \mathcal{O}(\varepsilon^{m+1}). \quad (\text{B.2})$$

Since the vector field is assumed to be sufficiently smooth, we may differentiate both sides of this equation with respect to x to obtain

$$Dh_m(\cdot) = \sum_{i=0}^m \varepsilon^i Dh_{[i]}(\cdot) + \mathcal{O}(\varepsilon^{m+1}). \quad (\text{B.3})$$

Combining Eqs. (B.1) and (B.3), then, we find

$$(D_z L_m)(\cdot, h_m(\cdot), \varepsilon) = C \left(- \sum_{i=0}^m \varepsilon^i Dh_{[i]}(\cdot) + \mathcal{O}(\varepsilon^{m+1}), I_{N_f} \right).$$

This equation shows that the rows of $(D_z L_m)(x, h_m(x), \varepsilon)$ span $N_z \mathcal{L}$ up to and including terms of $\mathcal{O}(\varepsilon^m)$. Hence, application of the one-higher-order proposition, Proposition A.1, completes the proof of this lemma. ■

Before we proceed with the proof of Lemma 2.2, we prove the following result which will be needed therein.

Lemma B.1 *For $m = 0, 1, \dots$, for $H = \mathcal{O}(\varepsilon)$, and for a general point $z = (x, y)$, the function L_m is written as*

$$L_m(z) = (-\varepsilon^{-1}H)^{m+1} [(D_y g)_0(z)]^m g_0(z) + \mathcal{O}(\varepsilon, \|g_0(z)\|^2),$$

where the notation “ $(\cdot)_0(z)$ ” stands for $(\cdot)(z, 0)$. The Jacobian $D_y L_m$ is written as

$$(D_y L_m)(z) = (-\varepsilon^{-1}H (D_y g)_0)^{m+1} + \mathcal{O}(\varepsilon, \|g_0(z)\|). \quad (\text{B.4})$$

Proof. For this proof, we write $(\cdot)_0$ instead of $(\cdot)_0(z)$ for the sake of brevity. The proof is by induction on m . For $m = 0$, we recall Eq. (2.4),

$$L_0 = -\varepsilon^{-1}H g,$$

and hence, expanding g in powers of ε , we find

$$L_0 = -\varepsilon^{-1}H g_0 + \mathcal{O}(\varepsilon).$$

This is the desired formula for L_0 . Differentiating both members of this formula with respect to y , we obtain

$$D_y L_0 = -\varepsilon^{-1}H (D_y g)_0 + \mathcal{O}(\varepsilon).$$

This is the desired formula for $D_y L_0$.

Next, we carry out the induction step for general m , namely we assume that

$$L_m = (-\varepsilon^{-1}H)^{m+1} (D_y g)_0^m g_0 + \mathcal{O}(\varepsilon, \|g_0\|^2), \quad (\text{B.5})$$

$$D_y L_m = (-\varepsilon^{-1}H (D_y g)_0)^{m+1} + \mathcal{O}(\varepsilon, \|g_0(z)\|) \quad (\text{B.6})$$

and show that

$$L_{m+1} = (-\varepsilon^{-1}H)^{m+2} (D_y g)_0^{m+1} g_0 + \mathcal{O}(\varepsilon, \|g_0\|^2). \quad (\text{B.7})$$

$$D_y L_{m+1} = (-\varepsilon^{-1}H (D_y g)_0)^{m+2} + \mathcal{O}(\varepsilon, \|g_0(z)\|). \quad (\text{B.8})$$

By Eq. (2.9),

$$L_{m+1} = -\varepsilon^{-1}H (D_z L_m) G = -\varepsilon^{-1}H [\varepsilon (D_x L_m) f + (D_y L_m) g],$$

Then, we substitute the induction hypothesis (B.5) into this expression. Application of the differential operator $(-H/\varepsilon)[\varepsilon (D_x \cdot) f + (D_y \cdot) g]$ on the $\mathcal{O}(\varepsilon, \|g_0\|^2)$ remainder

does not alter its asymptotic magnitude. Moreover, the term $\varepsilon(D_x L_m)f$ is $\mathcal{O}(\varepsilon)$ and, hence, can be absorbed also in the remainder. Therefore, we are left with the term $(-H/\varepsilon)(D_y L_m)g$. Substituting $D_y L_m$ into this expression from the induction hypothesis (B.6), we arrive at the desired formula (B.7).

Finally, we prove the leading order formula (B.8). First, we differentiate both members of the leading order formula (B.7) with respect to y and use the product rule derivative to evaluate the right member. The second term from the product rule is precisely the leading order term in Eq. (B.4). The other term from the product rule,

$$m(-\varepsilon^{-1}H)^{m+2}(D_y^2 g)_0((D_y g)_0^{m-1}, g_0),$$

may be absorbed in the remainder since it is linear in g_0 . Thus, we have obtained the desired formula (B.8) and completed the proof of the lemma. ■

Proof of Lemma 2.2. We first use [2, Theorem 3] to establish that condition (2.10) has a solution $y = h_{m+1}(x)$ which is $\mathcal{O}(\varepsilon^{m+1})$ -close to \tilde{h}_{m+1} . According to that theorem, it suffices to show that

$$\left((D_z L_m)(x, \tilde{h}_{m+1}(x), \varepsilon)\right) G(x, \tilde{h}_{m+1}(x), \varepsilon) = \mathcal{O}(\varepsilon^{m+2}).$$

By the definition of \tilde{h}_{m+1} ,

$$\left((D_z L_m)(\cdot, h_m(\cdot), \varepsilon)\right) G(\cdot, \tilde{h}_{m+1}(\cdot), \varepsilon) = 0.$$

Thus, we may write

$$\begin{aligned} & \left((D_z L_m)(\cdot, \tilde{h}_{m+1}(\cdot), \varepsilon)\right) G(\cdot, \tilde{h}_{m+1}(\cdot), \varepsilon) \\ &= \left[(D_z L_m)(\cdot, \tilde{h}_{m+1}(\cdot), \varepsilon) - (D_z L_m)(\cdot, h_m(\cdot), \varepsilon)\right] G(\cdot, \tilde{h}_{m+1}(\cdot), \varepsilon). \end{aligned} \quad (\text{B.9})$$

Next, we have the following estimates of the asymptotic magnitudes of the two terms in the right member of Eq. (B.9):

$$\tilde{h}_{m+1} = \sum_{i=0}^{m+1} \varepsilon^i h_{[i]} + \mathcal{O}(\varepsilon^{m+2})$$

by Lemma 2.1, and also

$$h_m = \sum_{i=0}^m \varepsilon^i h_{[i]} + \mathcal{O}(\varepsilon^{m+1})$$

by the induction hypothesis. Thus,

$$\tilde{h}_{m+1} - h_m = \mathcal{O}(\varepsilon^{m+1}),$$

and hence Taylor's Theorem with remainder yields

$$(D_z L_m)(\cdot, \tilde{h}_m + 1(\cdot), \varepsilon) - (D_z L_m)(\cdot, h_m(\cdot), \varepsilon) = \mathcal{O}(\varepsilon^{m+1}), \quad (\text{B.10})$$

since L_m and its derivatives are $\mathcal{O}(1)$. This is the desired estimate of the first term in the right member of Eq. (B.9).

It remains to estimate the second term, $G(\cdot, \tilde{h}_{m+1}(\cdot), \varepsilon)$ in the right member of Eq. (B.9). We recall that $G = \begin{pmatrix} \varepsilon f \\ g \end{pmatrix}$, where f and g are $\mathcal{O}(1)$ in general. Hence, the first component of $G(\cdot, \tilde{h}_{m+1}(\cdot), \varepsilon)$ is plainly $\mathcal{O}(\varepsilon)$. The second component is as well, since Lemma 2.1 implies that $\tilde{h}_{m+1,0} = h_{[0]}$ and hence that $g(\cdot, \tilde{h}_{m+1}(\cdot), \varepsilon) = \mathcal{O}(\varepsilon)$, also. Therefore,

$$G(\cdot, \tilde{h}_{m+1}(\cdot), \varepsilon) = \mathcal{O}(\varepsilon). \quad (\text{B.11})$$

Combining the estimates (B.10) and (B.11), we see that the right member of Eq. (B.9) is $\mathcal{O}(\varepsilon^{m+2})$, which is the desired result.

Finally, the solution of the condition $L_{m+1} = 0$ yields an N_s -dimensional manifold \mathcal{L}_{m+1} , as may be shown using the Implicit Function Theorem and [14, Theorem 1.13]. It suffices to show that

$$\det(D_y L_{m+1})(\cdot, h_{m+1}(\cdot)) \neq 0.$$

Lemma B.1 yields a leading order formula for $D_y L_{m+1}$,

$$(D_y L_{m+1})(z) = (-\varepsilon^{-1} H(D_y g)_0)^{m+2} + \mathcal{O}(\varepsilon, \|g_0(z)\|).$$

Here, z is a general point and $(\cdot)_0(z) = (\cdot)(z, 0)$. Next, we showed above that $h_{(m+1,0)} = h_0$. Recalling, then, Eq. (2.5), we obtain

$$(D_y L_{m+1})(x, h_{m+1}(x)) = [-\varepsilon^{-1} H(D_y g)_0]^{m+2} + \mathcal{O}(\varepsilon), \quad \text{for all } x \in K,$$

where $(D_y g)_0 = (D_y g)(x, h_0(x), 0)$. Thus,

$$\det(D_y L_{m+1})(x, h_{m+1}(x)) \neq 0, \quad \text{for all } x \in K,$$

by normal hyperbolicity and the proof is complete. ■

References

- [1] G. Browning, H.-O. Kreiss, Problems with different time scales for nonlinear partial differential equations, *SIAM J. Appl. Math.* **42(4)** (1982) 704–718
- [2] J. Carr, *Applications of Centre Manifold Theory*, Applied Mathematical Sciences, **35**, Springer–Verlag, New York, 1981
- [3] J. Curry, S. E. Haupt, M. E. Limber, Low-order modeling, initializations, and the slow manifold, *Tellus* **47A** (1995) 145–161
- [4] C. W. Gear, T. J. Kaper, I. G. Kevrekidis, and A. Zagaris, Projecting to a Slow Manifold: Singularly Perturbed Systems and Legacy Codes, *SIAM J. Appl. Dyn. Syst.* **4** (2005) 711–732
- [5] C. W. Gear and I. G. Kevrekidis, Constraint-defined manifolds: a legacy-code approach to low-dimensional computation, *J. Sci. Comp.*, **25(1)** (2005), 17–28
- [6] S. S. Girimaji, Reduction of large dynamical systems by minimization of evolution rate, *Phys. Rev. Lett.*, **82** (1999), 2282–2285
- [7] C. K. R. T. Jones, Geometric singular perturbation theory, in: *Dynamical Systems, Montecatini Terme*, L. Arnold, Lecture Notes in Mathematics, **1609**, Springer-Verlag, Berlin, 1994, pp. 44–118
- [8] H. G. Kaper and T. J. Kaper, Asymptotic analysis of two reduction methods for systems of chemical reactions, *Physica D* **165** (2002), 66–93
- [9] C. T. Kelley, *Iterative Methods for Linear and Nonlinear Equations*, Frontiers In Applied Mathematics, **16**, SIAM Publications, Philadelphia, 1995
- [10] I. G. Kevrekidis, C. W. Gear, J. M. Hyman, P. G. Kevrekidis, O. Runborg, and C. Theodoropoulos, Equation-free, coarse-grained multiscale computation: enabling microscopic simulators to perform system-level analysis, *Commun. Math. Sci.* **1** (2003) 715–762
- [11] H.-O. Kreiss, Problems with different time scales for ordinary differential equations, *SIAM J. Numer. Anal.* **16(6)** (1979) 980–998
- [12] H.-O. Kreiss, Problems with Different Time Scales, in *Multiple Time Scales*, J. H. Brackbill and B. I. Cohen, eds., Academic Press, 1985, pp. 29–57
- [13] E. N. Lorenz, Attractor sets and quasi-geostrophic equilibrium, *J. Atmos. Sci.* **37** (1980) 1685–1699
- [14] P. J. Olver, *Applications of Lie Groups to Differential Equations*, Graduate Texts in Mathematics, **107**, Springer–Verlag, New York, 1986

- [15] G. M. Shroff and H. B. Keller, Stabilization of unstable procedures: A recursive projection method, *SIAM J. Numer. Anal.* **30** (1993) 1099–1120
- [16] P. van Leemput, W. Vanroose, and D. Roose, Initialization of a Lattice Boltzmann Model with Constrained Runs, Report TW444, Catholic University of Leuven, 2005
- [17] P. van Leemput, C. Vandekerckhove, W. Vanroose, and D. Roose, Accuracy of hybrid Lattice Boltzmann/Finite Difference schemes for reaction-diffusion systems, *Multiscale Model. Sim.*, to appear
- [18] A. Zagaris, H. G. Kaper, and T. J. Kaper, Analysis of the Computational Singular Perturbation reduction method for chemical kinetics, *J. Nonlin. Sci.* **14** (2004) 59–91
- [19] A. Zagaris, H. G. Kaper, and T. J. Kaper, Fast and slow dynamics for the Computational Singular Perturbation method, *Multiscale Model. Sim.* **2** (4) (2004) 613–638